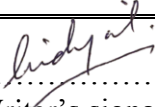




University of
Stavanger

Faculty of Science and Technology

MASTER'S THESIS

Study program/Specialization: Petroleum Geosciences Engineering	Spring semester, 2021 Open
Writer: Hidayat Ullah	 (Writer's signature)
Supervisors: Skule Strand Tina Puntervold Ivan Dario Pinerez Torrijos	
Thesis title: Optimization of a smart water composition for Enhanced Oil Recovery study by wettability alteration in carbonates at high temperature.	
Credits (ECTS): 30	
Key words: Wettability alteration Spontaneous Imbibition Smart Water Ion Chromatography Chalk/carbonates	Pages: 92 + enclosure: Stavanger, June 15, 2021

MASTER'S THESIS

Optimization of a smart water composition for Enhanced Oil Recovery study by wettability alteration in carbonates at high temperature.

By:

Hidayat Ullah



Universitetet
i Stavanger

FACULTY OF SCIENCE AND TECHNOLOGY
DEPARTMENT OF ENERGY RESOURCES

June 15, 2021

Abstract

Seawater due to its wettability modifying qualities has proved to be an excellent injection fluid in chalk. At high temperature seawater alter wettability towards more water-wet conditions thus improving the overall oil displacement by spontaneous imbibition into the chalk matrix. Smart Water is that injection brine which is specifically design to alter the wettability of reservoir towards the more water-wet state. Such kind of Smart Water needs to be abundant in concentration of some ions like Ca^{2+} , SO_4^{2-} , and Mg^{2+} .

In this research, finding efficient Smart Water's composition, concentration, and stable equilibrium are aimed. Stevns Klint Chalk cores used for their analogy importance to Ekofisk. Experiment temperature is also chosen as reservoir temperature of Ekofisk (130 °C) to provide a better resemblance to reservoir conditions.

Three cores were cleaned with de-ionized water, restored 10% Swi with sulfate-free formation water, and 90% Soi with oil with AN equal to 0.53 mg KOH/g. After that, two types of Smart Water i.e. Smart Water-1 (SmW-1) having composition of CaSO_4 (20mM) and MgCl_2 (20mM) and Smart Water-2 (SmW-2) having composition of CaSO_4 (20mM) and MgCl_2 (40mM) were prepared. Core No. 1 was spontaneously imbibed (SI) with Formation Water (FW) in secondary mode. SmW-1 was SI in tertiary mode and in secondary mode with Core No. 1 and Core No. 2 respectively while Core No. 3 was SI with SmW-2 in secondary model.

The results of spontaneous imbibition of Core #1 with FW confirms an ultimate recovery of 34 %OOIP reached after 4 days. Ultimate recovery of 55.5 %OOIP was reached by Core No. 1 after 43 days by SI of SmW-1 in tertiary mode. Core No. 2 reached ultimate recovery plateau of 66.1 %OOIP while Core No. 3 had an ultimate recovery plateau of 53.8 %OOIP in secondary mode.

Comparison of these results with Tahmiscioglu (2020), Andreassen (2019) and Lindanger (2019) shows that SmW-1 had more ultimate recovery of oil due to better alteration of wettability towards water-wet conditions than the Smart Water and Sea Water used by these other researchers.

Acknowledgments

First, I express an appreciation to associate professors Skule Strand and Tina Puntervold for their continuous support, supervision, encouragement, and motivation that made this research possible. I am thankful to them for giving me time to discuss my research and make me understand the work and improve my writing proficiency. This Smart Water EOR Group was a great learning experience for me.

I would like to extend my gratitude to Dr. Iv'an Dar'io Piñerez Torrijos for enlightening me with basic concepts as well as assistance in laboratory work.

Further, I want to thank my lab partner and Ph.D. fellow Muhammad Ashraful Islam Khan for providing a cultured environment filled with great discussions. His availability at the laboratory and knowledge of the instruments and procedures helped me a lot.

I also acknowledge the National IOR Centre for funding and collaboration.

Finally, I would like to thank my family, fellow students, and friends for their support and encouragement during this final semester.

Hidayat Ullah

List of Figures

Figure 3.1	Capillary tube redrawn after (Green and Willhite, 1998). The diameter of tube has been exaggerated for illustration purpose.....	10
Figure 3.2	Capillary tube in an oil/water system, redrawn after (Green and Willhite, 1998). The diameter of tube has been exaggerated for illustration purposes.....	11
Figure 3.3	Porous medium (simplified) as parallel capillary tube's pack (Lindanger, 2019).....	14
Figure 3.4	Displacement of oil by waterflooding for (a) oil-wet mineral surface (b) water wet mineral surface (Strand, 2005).....	16
Figure 3.5	The distribution of oil and water in a) a water-wet system and b) an oil-wet system. Redrawn after Ahr (2011).....	17
Figure 3.6	Measurement of contact angle (Green and Willhite, 1998).....	19
Figure 3.7	Spontaneous imbibition test's illustration. Red curve is showing sample core while green curve is representing reference core that is strongly water-wet.....	22
Figure 3.8	Amott and Harvey wettability test's capillary pressure curve (Tina Puntervold, 2008).....	24
Figure 3.9	Typical chromatography wettability result for a water-wet carbonate core.....	26
Figure 3.10	Illustration of SCN^- and SO_4^{-2} ions around water-wet carbonate mineral surface.....	26
Figure 3.11	Typical chromatography wettability result for an oil-wet carbonate core surface.....	26
Figure 3.12	Illustration of SCN^- and SO_4^{-2} ions around oil-wet carbonate mineral surface.....	26
Figure 4.1	Recovery of oil made at 120 °C by spontaneous imbibition and forced displacement successively (Strand et al., 2008).....	29
Figure 4.2	Tests of SI at 90 °C on chalk cores restored equally. Modified SW as Smart Water imbibing brines (Zhang, 2006).....	30
Figure 4.3	Test results of SI at 100 °C on chalk cores equally restored (Zhang, 2006).....	31
Figure 4.4	Test results of SI at 70 °C on chalk cores equally restored. Ca^+ concentration increase in SW imbibing brine (Zhang, 2006).....	32

Figure 4.5	Tests of SI tests done at different temperature of 70 °C, 100 °C and 130 °C with and without concentration of Calcium and Magnesium ions (Austad et al., 2007).....	33
Figure 4.6	Oil recovery at 90 °C by successive spontaneous imbibition and forced displacement.....	34
Figure 4.7	Oil recovery at 120 °C by successive spontaneous imbibition and forced displacement.....	34
Figure 4.8	Suggested wettability alteration mechanism with seawater. Figure from smart water group at University of Stavanger.....	35
Figure 5.1	Set-up for oil saturation establishment (Lindanger, 2019).....	45
Figure 5.2	Set-up used for Spontaneous Imbibition Test (Lindanger, 2019).....	46
Figure 6.1	Comparison of Ca precipitation of CaSO ₄ with MgCl ₂ (1:1) (left) and NaSO ₄ with CaCl ₂ (1:1) (right) solutions at 130 °C.....	48
Figure 6.2	Ca precipitation of CaSO ₄ and MgCl ₂ (1:2) solution at 130 °C.....	48
Figure 6.3	Ca precipitation of CaSO ₄ and MgCl ₂ (1:3) solution at 130 °C.....	49
Figure 6.4	Vials containing different concentration solutions of CaSO ₄ and MgCl ₂	50
Figure 6.5	Vials containing solutions of CaSO ₄ and MgCl ₂ (having different concentration of NaHCO ₃).....	50
Figure 6.6	Vials containing different concentration solutions of NaSO ₄ and CaCl ₂	51
Figure 6.7	Ion Chromatography results of brines with different molar concentration at room temperature.....	52
Figure 6.8	Ion Chromatography results of brines with different molar concentration after 130 °C.....	53
Figure 6.9	Ion Chromatography results of brines with different molar concentration with NaHCO ₃ at room temperature.....	54
Figure 6.10	Ion Chromatography results of brines with different molar concentration with NaHCO ₃ after 130 °C.....	54
Figure 6.11	Batch test for presence of SO ₄ ²⁻ ions in effluent samples. Ba ²⁺ ions added confirming formation of BaSO ₄	55
Figure 6.12	Oil recovery with spontaneous imbibition of Core#1 with FW at 130 °C.....	58
Figure 6.13	Oil recovery with spontaneous imbibition of Core#1 with FW and SmW-1 (containing 20 mM Ca ²⁺ , 20 mM SO ₄ ²⁻ , and 20mM Mg ²⁺) at 130 °C.....	59
Figure 6.14	Oil recovery with spontaneous imbibition of Core#2 with SmW-1 at 130 °C.....	60

Figure 6.15	Oil recovery with spontaneous imbibition of Core#3 with SmW-2 (containing 20 mM Ca ²⁺ , 20 mM SO ₄ ²⁻ , and 40mM Mg ²⁺) at 130 °C	61
Figure 6.16	SI test results performed in a strongly water-wet SK Chalk Core (Tahmiscioglu, 2020) restored with Swi =10% and saturated with heptane...	62
Figure 7.1	Comparison of effect of FW and SmW-1 in secondary and tertiary mode at 130 °C.....	65
Figure 7.2	Comparison of effect of SmW-1 and SmW-2 in secondary and tertiary mode at 130 °C.....	66
Figure 7.3	Oil Recovery with SI by FW and 10 mM CaSO ₄ in Core #1 at 130 °C (Tahmiscioglu, 2020).....	67
Figure 7.4	Oil Recovery with SI by 10 mM CaSO ₄ at 130°C (Tahmiscioglu, 2020).....	68
Figure 7.5	Oil Recovery with SI by FW-SW in Core#6 at 130°C (Tahmiscioglu, 2020).....	68
Figure 7.6	Oil Recovery with SI by SW in Core #2 at 130°C (Tahmiscioglu, 2020).....	69
Figure 7.7	Oil Recovery with SI by Smart Water 13 mM CaSO ₄ at 70 °C in Core #SK4 (Andreassen, 2019).....	70
Figure 7.8	Oil Recovery with SI by SW at 70°C in Core #SK3 (Andreassen, 2019).....	71
Figure 7.9	Oil Recovery with SI by Smart Water in Core #SK6 at 90 °C (Lindanger, 2019).....	72
Figure 7.10	Oil Recovery with SI by SW in Core #SK5 at 90 °C (Lindanger, 2019).....	73

List of Tables

Table 3.1	Classification of EOR Methods.....	5
Table 3.2	Wettability states for the range of contact angles.....	20
Table 3.3	Amott Harvey index for different wetting states.....	25
Table 3.4	Wettability states for the wettability index value.....	27
Table 5.1	Measured Properties of Three Studied Cores.....	36
Table 5.2	Measured Properties of Oil.....	38
Table 5.3	Brine Compositions and Properties.....	40
Table 6.1	pH of the brines of CaSO ₄ and MgCl ₂ with and without NaHCO ₃ and brine of CaCl ₂ and NaSO ₄	47
Table 6.2	Ion Chromatography results of brines with different molar concentration at room temperature and at 130 °C.....	52
Table 6.3	Ion Chromatography results of brines with different molar concentration with NaHCO ₃ at room temperature and at 130 °C.....	53
Table 6.4	Results of Porosity Measurement.....	56
Table 6.5	Results of Permeability Measurement.....	57
Table 6.6	Modified Indices values for all three cores.....	63
Table 7.1	Comparison of Secondary and Tertiary recovery results of the current study with Tahmiscioglu (2020) work at 130°C	67
Table 7.2	Comparison of Secondary recovery results of the current study with Andreassen (2019) work	70
Table 7.3	Comparison of Secondary recovery results of the current study with Lindanger (2019) work	71

Abstract	(i)
Acknowledgements	(ii)
List of Figures	(iii)
List of Tables	(vi)
1 Introduction	1
2 Objectives	2
3 Theory	3
3.1 Carbonate Reservoirs	3
3.2 Oil Recovery in Carbonate Rocks	3
3.3 Enhanced Oil Recovery	4
3.4 Displacement Efficiencies and Forces	6
3.4.1 Microscopic and Macroscopic Displacement	6
3.4.2 Fluid Flow in Porous Media	7
3.4.3 Capillary Forces	10
3.4.4 Gravity Forces	13
3.4.5 Viscous Forces	14
3.4.6 Capillary Number	14
3.5 Wettability	15
3.5.1 Wettability in Porous Media	15
3.5.2 Effects of Wettability	18
3.5.3 Wettability in Carbonates	18
3.6 Wettability Measurement	19
3.6.1 Contact Angle Measurement	19
3.6.2 Spontaneous Imbibition	21
3.6.3 Amott Method	22
3.6.4 Amott-Harvey method	23
3.6.5 Chromatographic Wettability Test	25
4 Water-Based EOR in Carbonates	28
4.1 Waterflooding	28

4.2	Wettability Alteration in Carbonate by Modifying the Ionic Composition of Water	28
4.2.1	Na ⁺ Effect	30
4.2.2	SO ₄ ²⁻ Effect	30
4.2.3	Ca ⁺² Effect	31
4.2.4	Mg ⁺² Effect	32
4.2.5	Temperature Effect	33
4.3	Smart Water	34
5	Experimental Work	36
5.1	Materials	36
5.1.1	Core Material	36
5.1.2	Selection of Crude Oil	36
5.1.2.1	RES-40 Preparation	37
5.1.2.2	RES-40-Zero Preparation	37
5.1.2.3	Oil-A Preparation	37
5.1.3	Compounds	38
5.1.3.1	Calcium Sulphate (CaSO ₄)	38
5.1.3.2	Magnesium Chloride (MgCl ₂)	38
5.1.4	Brines	38
5.1.4.1	Preparation of Brines	38
5.1.4.2	Valhall Formation Brine FW (VB0S)	39
5.1.4.3	Smart Water	39
5.1.4.3.1	Smart Water-1 (SmW-1)	39
5.1.4.3.2	Smart Water-2 (SmW-2)	39
5.2	Analysis	40
5.2.1	pH Measurement	40
5.2.2	PHREEQC	40
5.2.3	Temperature stability of brine	41
5.2.3.1	Bulk Test Analyses	41
5.2.3.2	Ion Chromatography Analyses of Brines	41
5.3	Methodology	41
5.3.1	Core Cleaning	41
5.3.2	Porosity Measurement	42

5.3.3	Permeability Measurement	43
5.3.4	Core Restoration for Spontaneous Imbibition Experiments	44
5.3.4.1	Establishing Initial Water Saturation	44
5.3.4.2	Establishing Oil Saturation	45
5.3.4.3	Ageing	45
5.3.5	Oil Recovery by Spontaneous Imbibition Test	45
5.3.6	Selection of Optimum Brine with respect to Precipitation	46
6	Results	47
6.1	pH Measurement	47
6.2	PHREEQC	47
6.3	Temperature stability of Brine	49
6.3.1	Bulk test analyses	49
6.3.2	Chemical analyses of brines using Ion Chromatography	51
6.4	Core Cleaning	54
6.5	Porosity and Permeability Measurement	55
6.5.1	Porosity Measurement	55
6.5.2	Permeability Measurement	56
6.6	Initial core wettability	57
6.7	Effect of Smart Water-1 in tertiary recovery mode	58
6.8	Effect of Smart Water-1 in secondary mode	59
6.9	Effect of Smart Water-2 in secondary mode	60
6.10	Wettability Measurement	61
7	Discussions	64
7.1	Effect of brine composition on wettability alteration	66
7.2	Reactivity effect of temperature and brine composition	69
8	Conclusion	74
8.1	Future Work	75
	Bibliography	76
	Appendixes	80

1 Introduction

The energy demand of the world is increasing at a rapid pace, and meeting this ever-growing demand, hydrocarbons play an essential role. Their extraction does have an adverse effect on the environment, but their economic impact cannot be neglected as well.

Extracting hydrocarbons is not a cost-effective method and with the increase in the usage of new technologies as well as harsh conditions of the newly developing fields increase the cost of producing well by multifold. This high cost of new wells leads to an increase in the importance of already producing fields that have proven reserves of hydrocarbon in them. To achieve the task of producing hydrocarbons economically, it is essential to focus on the increase in the rate of oil recovery.

Carbonate reservoirs are enriched in oil, and they contain approximately 50 percent of the total world's oil reserves. Comparing to the sandstone reservoirs, the oil recovery in carbonate is generally low that is less than 30 percent, and around 70 percent of the oil got left in the carbonate. This low rate of recovery is generally due to the fact that 90 percent of carbonates are mixed wet to oil-wet and because of carbonates' fractured nature. Negative capillary forces get promoted by the preceding two factors, which leads to the prevention of oil displacement by water in the reservoir. Moreover, non-homogenous and low matrix permeability are the other two factors that impact the recovery of oil in carbonates as well (Austad et al., 2007).

These all factors in carbonates create a potential for research in enhanced oil recovery (EOR) methods. So, chemical enhanced oil recovery techniques have been researched widely and carefully. Polymers have an adverse impact on the environment, so in this research, non-polymers have been used, and their impact on the enhanced oil recovery has been monitored. This research has been carried out to improve the sea water alteration by changing ions to increase ultimate recovery of oil.

2 Objectives

This thesis study aims to change the wettability of chalk carbonates at a temperature of 130°C by changing the ionic composition of injection brine known as "Smart Water." The goal of the study is to use this "Smart Water" to alter the wettability of chalk, to move from a more mixed-wet to more water-wet state with the help of changing different ions such as SO_4^{2-} , Ca^{2+} and Mg^{2+} which makes water imbibe into smaller pores in carbonates. This imbibition increases the microscopic sweep efficiency of the injection brine resulting in better Enhanced Oil Recovery (EOR) at high temperature of 130 °C.

Another target of the study is to look for the ion concentration and composition of Smart Water that does not cause any precipitation in water, rock, and brine to produce the best wettability modifier i.e., Smart Water.

Furthermore, this research finds the effect of Formation Water and then Smart Water on oil recovery performance in both secondary mode and tertiary mode.

The study also aims to compare the results of oil recovery performance of both Smart Water and Formation Water by Spontaneous Imbibition in secondary as well as tertiary modes. Then compare the results of EOR of Smart Water with already available results of sea water and Smart Water of Tahmiscioglu (2020), Andreassen (2019) and Lindanger (2019).

3 Theory

3.1 Carbonate Reservoirs

Carbonate rocks are those kinds of sedimentary rocks which are formed by the processes like accumulation and then lithification of carbonate materials, and these materials have been precipitated by a different type of animals, plants and other organisms etc. Carbonate rocks fall in the category of biogenic rocks due to their formation from living organisms or the products made from living organisms. Calcium (Ca^{2+}) and carbonate (CO_3^{2-}) are two types of ions that are present in large amounts in seawater in dissolved form; microorganisms convert these two ions into carbonate minerals (Grotzinger and Jordan, 2014).

Carbonate minerals consist of different carbonate minerals like Dolomite (CaMgCO_3), Calcite (CaCO_3), Aragonite (CaCO_3), Ankerite ($\text{CaFe}(\text{CO}_3)_2$), Magnesite (MgCO_3), and Siderite (FeCO_3) (Punternold, 2008). The ionic composition of aragonite and calcite is the same, but they have different structures. Calcite and dolomite are the chief minerals present in most carbonate sedimentary rocks. Limestone is that carbonate rock that is made up of calcite, while dolomite dominant rock is known as dolostone (Grotzinger and Jordan, 2014). Carbonate reservoir in the world holds half of the world's reserves of petroleum (Treiber & Owens, 1972).

This research is based on the carbonate rock known as chalk. Chalk is composed mainly of the deposits of marine foraminifera and marine algae known as coccolithophorid. It is fine-grained, porous, friable, soft, and permeable rock. Homogeneity is significantly less in chalk, so it does not depict high permeability.

3.2 Oil Recovery in Carbonate Rocks

Production of oil through wells has been completed in generally three different stages known as primary, secondary, and tertiary recovery. Primary recovery of hydrocarbons is made through the energy which is already stored in the reservoirs. This energy is due to the one or combination of more than one drive mechanism, i.e., fluid expansion, gravity drive, solution gas drive, aquifer

expansion, gas cap drive, or rock expansion etc. (Green & Willhite, 1998). These all processes deplete the pressure of the reservoir, so this type of recovery is as known as pressure depletion (Muskat, 1949).

The second type of recovery is known as secondary recovery. This recovery is needed when the pressure of reservoirs gets depleted due to the loss of pressure in primary recovery, and to continue the production, pressure support is required. This loss pressure is maintained mostly via the injection of gas or water. Different other types of fluids can also be used for the displacement of oil in the direction of wells that were already producing (Green & Willhite, 1998). The energy which is provided by this process increases the life of producing wells. This secondary recovery has the average range of recovery of original oil in place around 20 to 40 percent (Muggeridge et al., 2014).

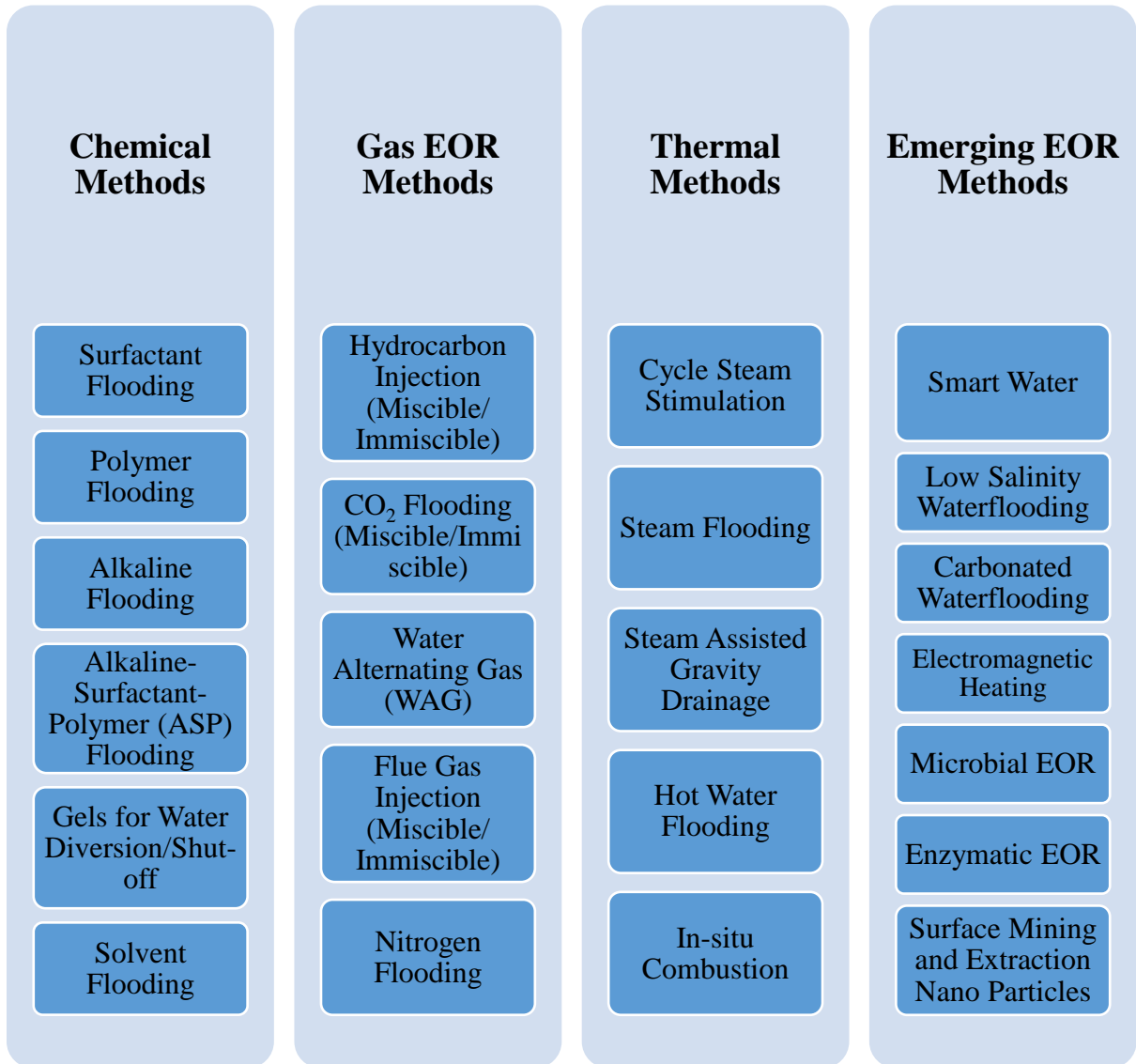
The third stage of recovery is known as tertiary recovery or tertiary production. Tertiary production does not mean that this recovery is required after primary and secondary recovery. In some cases like for instance, in heavy oil cases, tertiary recovery (thermal energy) is needed from the very start of the production processes, so it is more appropriate to call this type of recovery as Enhanced Oil Recovery (EOR). The main objective of the EOR is to improve or enhance the sweep efficiency for extracting the hydrocarbons that were left behind in the first two stages. Fluid is injected, which interacts with the rock and oil, which as a result, increases the overall recovery. EOR is categorized into the following categories: miscible, immiscible gas drives, chemical, thermal and other (Green and Willhite, 1998).

3.3 Enhanced Oil Recovery

The main purpose of EOR is to extract more oil than was already left in the field due to a decline in production. Exploration expenditure has been saved substantially due to working on the already producing fields in the case of EOR. The world that has usage of 31.6 percent of oil out of total global energy. EOR still has relatively high importance in the industry that is finding it difficult to discover new giant oil reserves (Cook, 2013). With the passage of time, several researchers with different backgrounds have given different EOR solutions with working on either reduction of

mobility ratio, interfacial tension, and alteration of wettability to increase the oil recovery. Table 3.1 classifies these EOR methods under four categories (Torrijos et al., 2019).

Table 3.1-Classification of EOR Methods



3.4 Displacement Efficiencies and Forces

3.4.1 Microscopic and Macroscopic Displacement

The product of two different types of displacement efficiencies, i.e., microscopic displacement efficiency and macroscopic displacement efficiency, are known as total displacement efficiency. Overall displacement efficiency is expressed in Equation 3.1 below:

$$E = EDEv \quad 3.1$$

Where

- E , Efficiency of Total displacement
- ED , Efficiency of Microscopic displacement
- Ev , Efficiency of Macroscopic displacement

Above equation 3.1 represents that when Total displacement efficiency (E) gets closer to 1, then the oil displacement efficiency will be higher. In the above equation, ED is directly related to residual oil saturation, and it shows oil mobilization at pore scale while Ev is the measure of the effectiveness of EOR agent at its making connection with pore volume (Green and Willhite, 1998).

Enhanced oil recovery processes decrease the residual oil saturation and increase microscopic displacement efficiency. Chemical and physical reactions between water, oil, and rock dictate the residual oil saturation (S_{or}); ED is increased, and S_{or} is decreased on the basis of alteration wettability and interfacial tension (IFT). Equation 3.2 shows how microscopic displacement efficiency (ED) and residual oil saturation (S_{or}) relates.

$$ED = \frac{S_{oi} - S_{or}}{S_{oi}} \quad 3.2$$

Where

- ED , Efficiency of Microscopic displacement
- S_{oi} , Saturation of Initial oil
- S_{or} , Saturation of Residual oil

Contrary, E_v is the result of several macro factors like structure and geometry of reservoir, viscosity ratio, and displaced and displacing fluids' density. Early water breakthrough occurs due to poor flooding performance and high mobility ratio, which is the result of viscosity differences, high density of reservoir, and an unfavorable geometry of reservoir. Ideally, to have a late water breakthrough low mobility ratio is necessary, which is created by making a uniform flood front by the studying ED.

3.4.2 Fluid Flow in Porous Media

In the 1850s, Henry Darcy experimented on fluid flow via sand packs and formulated an equation known as Darcy's law. He concluded that pressure drop, and the flow rate was proportional across sand pack while, on the other hand, viscosity is inversely proportional to them. He also observed that constant permeability (k) depends on filters on sand packs and gets varied by changing them. Permeability, when defined in terms of the reservoir, is the ease at which the fluid can pass through a certain formation, and it is expressed by Equation 3.3 below:

$$q = -\frac{Ak}{\mu} \frac{dp}{dx} \quad 3.3$$

Where

- q , flow rate
- A , the cross-sectional area
- μ , viscosity of the fluid
- k , permeability
- dp/dx , the pressure gradient

The above equation is valid for some cases, like if the flow is horizontal and fluid is incompressible and porous media is 100 percent saturated. The validity of the equation occurs when the flow is laminar, and there are no reactions chemically between porous media and the flowing fluid (Zolotukhin, 2000).

In the case of waterflooding, oil is being displaced by water, fluid's viscosities and wettability determine the mobility of the phase when there is another phase present as well (Torrijos et al., 2019). Mobility of water is represented by Equation 3.4, while the mobility of oil is represented by Equation 3.5 below.

$$\lambda_w = \frac{k_{rw}}{\mu_w} S_{or} \quad 3.4$$

$$\lambda_o = \frac{k_{ro}}{\mu_o} S_{or} \quad 3.5$$

Where

λ_w	Mobility of water (m ² / Pa.s)
λ_o	Mobility of oil (m ² / Pa.s)
k_{rw}	Relative permeability of water (fraction)
μ_w	Viscosity of water (Pa.s)
k_{ro}	Relative permeability of oil (fraction)
μ_o	Viscosity of oil (Pa.s)
S_{or}	Residual oil saturation (fraction)
S_{wi}	Irreducible water saturation (fraction)

Mobility factor (M) expressed in Equation 3.6 below is an essential aspect in the displacement of oil and porous media's fluid flow.

$$M = \frac{\lambda_D}{\lambda_d} = \frac{\lambda_w}{\lambda_o} = \frac{k_{rw}}{\mu_w} S_{or} = \frac{k_{ro}}{\mu_o} S_{wi} \quad 3.6$$

Where

M	Motility ration (fraction)
λ_D	Mobility of displacing fluid (m ² / Pa.s)

λ_d	Mobility of displaced fluid (m ² / Pa.s)
λ_w	Mobility of water (m ² / Pa.s)
λ_o	Mobility of oil (m ² / Pa.s)
k_{rw}	Relative permeability of water (fraction)
k_{ro}	Relative permeability of oil (fraction)
μ_w	Water's viscosity (Pa.s)
μ_o	Oil's viscosity (Pa.s)
S_{or}	Residual oil saturation (fraction)
S_{wi}	Irreducible water saturation (fraction)

The above factor describes the relative mobility of water and oil. In an ideal situation, water will be behind oil and displaces it in the manner of a piston. This preceding situation occurs when the mobility factor is less than 1. On the other hand, when the value of the mobility factor is greater than 1, then the process known as viscous fingering occurs, which results in a poor displacement process. Water flooding will be less effective when viscous fingering occurs because of water bypassing oil without displacing it.

In carbonate reservoirs that are fractured, the recovery mechanism is ruled by spontaneous imbibition, and efficiency is determined by the mineral surface's wettability. In the case of the oil-wet system, capillary pressure is present, which does the work against displacement of oil; in this scenario, imbibing fluid has to overcome the capillary entry pressure to the matrix. The Leverett J-function has a claim to calculate the capillary entry pressure given in Equation 3.7 below.

$$P_c = \sigma \sqrt{\frac{\bar{\phi}}{k}} J^* \quad 3.7$$

Where

P_c	Capillary pressure (Pa)
σ	Interfacial tension (N/m)

- ϕ Porosity (fraction)
- J^* Leverett dimensionless entry pressure ($J^* \approx 0.25$ for completely water wet)

3.4.3 Capillary Forces

It is the force that is determined by the displacement and fluid distribution in the reservoir. These forces get affected by the pore throat's dimensions and geometry, interfacial tension, and wettability. Displacement of oil, distribution of fluids, and fluid saturations are impacted directly by several forces like throat size of pore, rock mineral, and oil and water's interface surface energy (Green and Willhite, 1998).

When we place a capillary tube inside the container filled with water, then the water will draw up without any support externally as seen in Figure 3.1 below.

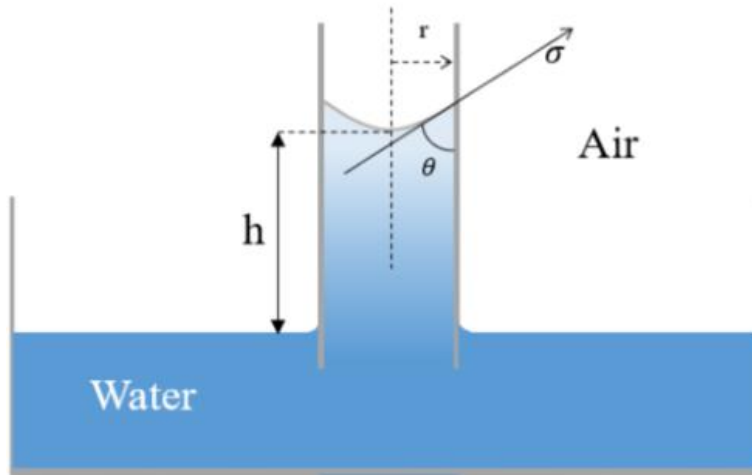


Figure 3.1 Capillary tube redrawn after (Green and Willhite, 1998). The diameter of the tube has been exaggerated for illustration purpose

The rise of water will continue until the weight of the water column neutralizes these capillary forces below the interface. When the equilibrium is attained by the system, then the sum of vertical forces (ΣF_y) must equal to zero. And this can be used to measure the surface tension (σ) from Equation 3.8 below:

$$\sigma \cos\theta 2\pi r = \pi r^2(\rho_w - \rho_a)gh \quad 3.8$$

θ the contact angle between the capillary tube and the water,

r the radius of the tube in cm.

h The height from free water level to meniscus

ρ_w Density of water in g/cm³

ρ_a Density of air in g/cm³

g Gravity constant in cm/s²

Then by expressing the equation in terms of the surface tension (σ), we get the following equation 3.9, with unit dynes/cm:

$$\sigma = \frac{rh(\rho_w - \rho_a)g}{2\cos\theta} \quad 3.9$$

The new system having oil, water and air is introduced to the study system in Figure 3.2 below at static conditions. To look for capillary pressure's expression, a force balance that is simple can be used as seen in Figure 3.2.

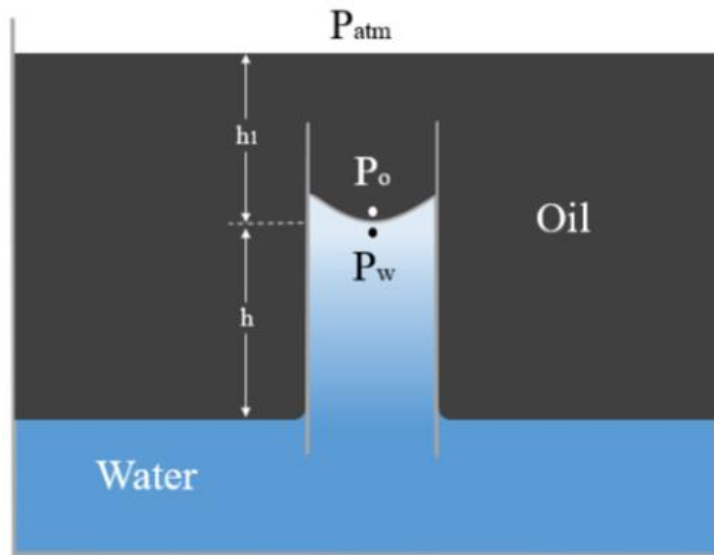


Figure 3.2 Capillary tube in an oil/water system, redrawn after (Green and Willhite, 1998).
The diameter of the tube has been exaggerated for illustration purposes

The pressure in the oil phase at the point above the interface is given in Equation 3.10 and water phase in Equation 3.11 as,

$$P_o = P_{atm} + \rho_o g h_1 \quad 3.10$$

$$P_w = P_{atm} + \rho_o g (h_1 + h) - \rho_w g h \quad 3.11$$

- P_{atm} the atmospheric pressure dynes/cm²
 h_1 the height from the surface to the interface in cm,
 h the height from interface down to the free water level in cm.
 ρ_o the density of oil in g/cm³
 ρ_w the density of water in g/cm³
 g the gravity acceleration constant in cm/s²

By taking the difference between the oil and water pressure resultant is Equation 3.12:

$$P_o - P_w = (P_{atm} + \rho_o g h_1) - (\rho_o g (h_1 + h) - \rho_w g h) \quad 3.12$$

The following Equation 3.13 becomes

$$P_o - P_w = (\rho_w - \rho_o) g h \quad 3.13$$

Capillary Pressure (P_c) is the pressure difference that exists between water and oil. By utilizing Equation 3.9, and keeping in mind that instead of air non-wetting phase is oil then we can solve this equation in terms of the water and oil density difference ($\rho_w - \rho_o$) and put it in Equation 3.13, and we get Equation 3.14:

$$P_c = \frac{2\sigma_{ow} \cos\theta}{r} \quad 3.14$$

Capillary forces act differently in the case of fractured and non-fractured reservoirs. Capillary forces in fractured reservoirs favor oil displacement, while the increase in residual oil saturation and oil trapping occurs in non-fractured reservoirs. This is expressed by Equation 3.15 below:

$$P_c = P_{NW} - P_W = \frac{2\sigma\cos\theta}{r} \quad 3.15$$

Where

P_c ,	Capillary pressure (Pa)
P_{NW} ,	The pressure of the non-wetting phase (Pa)
P_W ,	The pressure of the wetting phase (Pa)
σ ,	Interfacial tension between wetting and non-wetting phase (N/m)
θ ,	Contact angle (degree)
r ,	Pore radius (m)

3.4.4 Gravity Forces

These forces play quite an essential role in the movement of oil, especially in the case of tilted reservoirs. If the migration of oil is steep, then this can cause segregation of oil and gas due to their difference in density. Consequently, the produced oil will have lower gas to oil ratio, and the energy present in the reservoir will stay conserved for more time (Hall, 1961). Gravity forces play an important role in the flow of oil during two cases; firstly, when there is low interfacial tension between water and oil; and secondly, in case of an increase in the height of matrix that contains reservoir fluids (Austad and Milter, 1997). ΔP_g (pressure difference between oil and water) is expressed in Equation 3.16 below:

$$\Delta P_g = \Delta\rho gH \quad 3.16$$

Where

$\Delta\rho$	difference in density between oil and water (kg/m^3)
g	acceleration due to gravity (m/s^2)
H	height of the liquid column (m)

3.4.5 Viscous Forces

These are the forces that are calculated by the pressure gradient caused by the movement of fluid flowing across porous media (Green and Willhite, 1998). The simple way of calculating the value of viscous forces across any reservoir is that to think of the rock as he parallels capillary tubes' cluster and assume that the flow across these parallel tubes is laminar as seen in Figure 3.3. The pressure drop occurring in the single pipe for laminar flow is calculated using the Poiseuille's law in Equation 3.17.

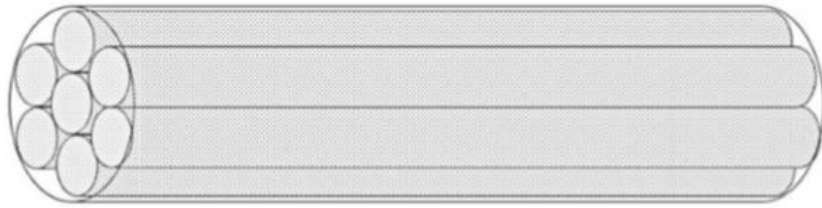


Figure 3.3 Porous medium (simplified) as parallel capillary tube's pack (Lindanger, 2019)

$$\Delta P = - \frac{8 \mu \Delta x v_{avg}}{r^2 g_c} \quad 3.17$$

Where

ΔP	Pressure drop across pipe (Pa)
μ	Viscosity of fluid (Pa.s)
Δx	Length of pipe (m)
v_{avg}	Average fluid velocity through the pipe (m/s)
r	Radius of pipe (m)
g_c	Conversion factor

3.4.6 Capillary Number

The capillary number that is represented by N_c is the ratio between capillary and viscous forces and is the dimensionless ratio. If the porous flow is dominated by viscous forces, then the value of capillary number will increase, which will lead to a decrease in residual oil saturation. The capillary number will decrease if the flow gets dominated by capillary force. The smaller capillary

number also indicates that oil that is present is capillary trapped, and saturation of residual oil increases. The capillary number is calculated through Equation 3.18 below (Moore & Slobod, 1955).

$$N_c = \frac{\mu_w v_o}{\sigma_{ow} \cos\theta} \quad 3.18$$

Where,

μ_w	Water viscosity (mPa.s)
v_o	Velocity (m/s)
σ_{ow}	Surface tension between oil and water (mN/m)
θ	Contact angle (degree)

3.5 Wettability

It is the tendency of the fluid to spread on the surface of solid rock in the presence of the other fluid, which is immiscible (Craig, 1971). Fluid distribution in porous media and properties of multiphase flow has been affected majorly by wettability. Wettability has an impact on the capillary pressure, curves of permeability, and saturation of residual oil, which leads to change in displacement efficiencies (Anderson, 2013). Oil recovery can be improved by altering the wettability in such a way that it can improve the efficiencies of oil displacement. Mineral surface's behavior for a certain type of fluid can be affected by temperature, aging, and surface charge (Strand, 2005).

3.5.1 Wettability in Porous Media

In the case of petroleum studies, wettability is hypothesized to occur between two extremes, i.e., either strongly water-wet or strongly oil-wet in the presence of oil and water that are two immiscible fluids. Unavailability of oil in porous sedimentary medium leads to the concept that this medium is water-wet originally. After the migration of oil occurs, the factors which were determining the state of wettability of the medium will change, and equilibrium will get established, and at that point reservoir's initial wettability state has been established.

The mineral surface's behavior against wettability is not the same throughout due to non-homogeneity across the reservoir. The rock does have heterogeneous wettability, which is due to different minerals in the rock having different specific affinity to oil or water. This change in wettability in the rock makes the partly water-wet and partly oil-wet.

The thin layer of oil will get established on the surface of the mineral in the case of the porous rock system, which is strongly oil-wet. Small pores will get filled by oil, and this forces the water to move towards larger pores and fill them as seen in Figure 3.4.

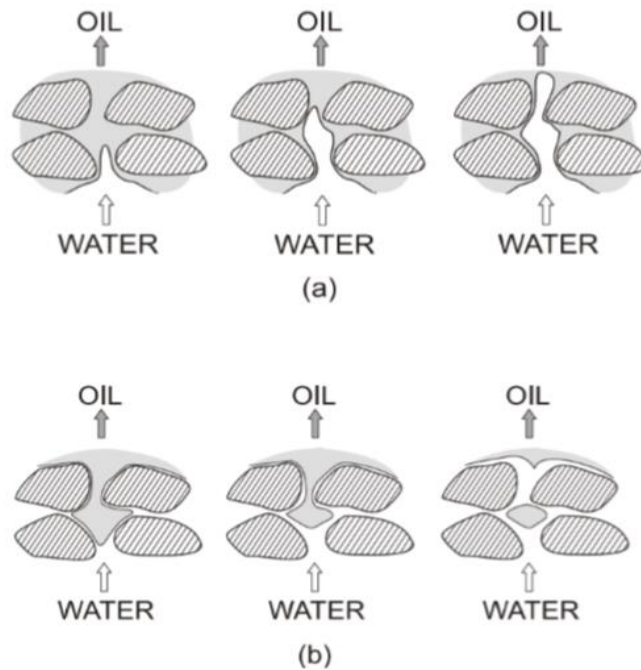


Figure 3.4 Displacement of oil by waterflooding for (a) oil-wet mineral surface (b) water wet mineral surface (Strand, 2005)

On the other hand, the porous system is highly water-wet; in that scenario, most of the rock's surface is filled by water and small pores as well, which made the oil move towards larger pores. In case of water flooding, the higher volume of oil will get trapped in larger pores Figure 3.5 (Ahr 2011).

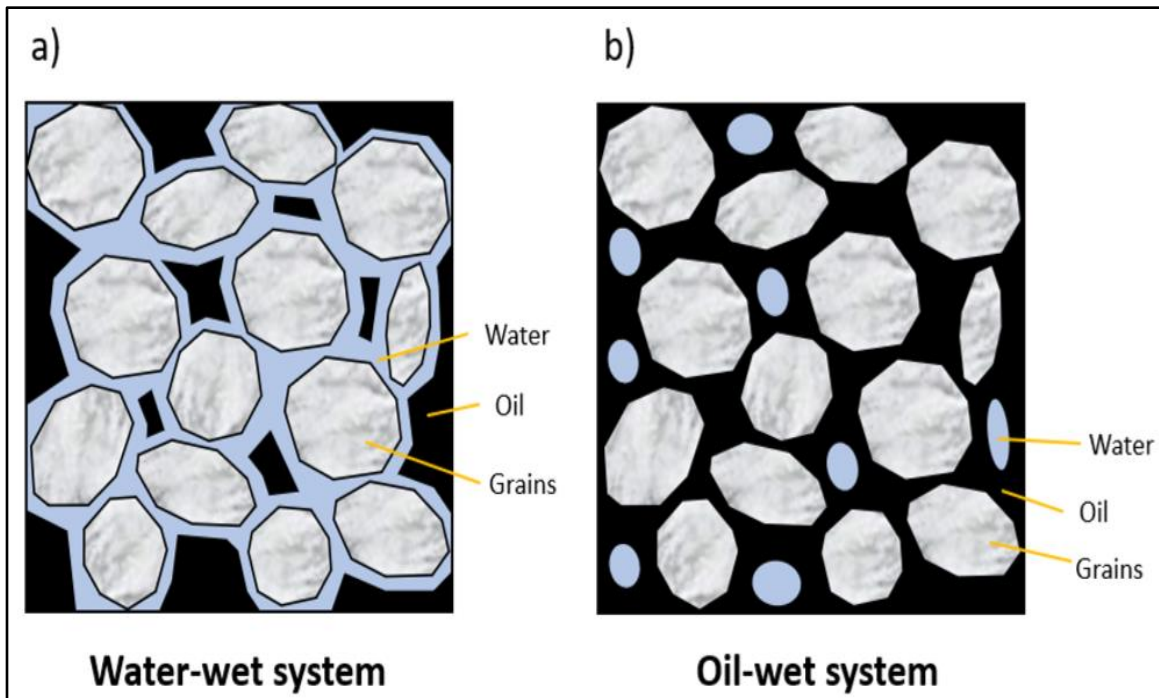


Figure 3.5 The distribution of oil and water in a) a water-wet system and b) an oil-wet system.

Redrawn after Ahr (2011)

The mineral composition of rock and crude oil components are the two most important factors that determine a porous system's wettability profile. If crude oil contains a higher amount of resin groups or asphaltene, this will affect the wetting due to the presence of polar molecules with basic or acidic nature (Anderson, 1986; Buckley, 1996). Polar components are differently present in carbonates and sandstone, showing different interactions and thus different wetting properties (Buckley & Liu, 1998).

Negatively charged ions will get attracted by carbonate minerals because they have a positively charged surface with a pH below the value of 8 to 9. The surface of minerals will become more oil-wet if they adsorb acidic oil components that are negatively charged (Pierre et al., 1990). On the other hand, the surface of sandstone minerals will be more oil-wet because, on the contrary, it absorbs more positively charged ions of basic oil components that have a value of pH above 2 (Menezes et al., 1989, Kowalewski et al., 2003).

3.5.2 Effects of Wettability

It is quite important to understand the porous system's wettability because this has some critical type of effects on different mechanisms phase trapping, fluid distribution, and multiphase flow. Wetting impacts other factors and directly affects irreducible saturation, relative permeability, capillary pressure, electrical properties, and several other processes related to EOR (Strand, 2005).

3.5.3 Wettability in Carbonates

Initially, most of the reservoir minerals in the porous system are strongly water-wet because of polar components' absence. Although, several factors along with oil intrusions change the wettability profile of the system and set the initial wettability to water or oil for rock minerals. Carbonate minerals have such characteristics of minerals that they are neutral to oil-wet (Treiber & Owens, 1972, Chilingar & Yen, 1983). The fracturing nature of carbonate reservoirs is another challenge other than being oil-wet. In reservoirs that are oil-wet, the dominant flow of fluid will be through fracture networks that are highly permeable while matrix blocks which are tight are isolated flow-wise, and oil stays in them due to the presence of strong capillary forces. As a result of this imbibition of injection, water does not occur sufficiently to the matrix of rock that is oil-bearing. In these kinds of reservoirs, the function of injection water is not as efficient as it is in reservoir systems that are water-wet (Strand, 2005).

Determination of wettability occurs on the basis of several parameters and different factors (Standnes, 2001). These factors include the mineral composition of the rock, crude oil's polar components, surface charge and polar oil components' water solubility (Buckley et al., 2013), potential determining ions' concentration and salinity of brine (Buckley, 1996), disjoining pressure, thin-film forces and capillary pressure (Hirasaki, 1991), pressure, oil's ability to stabilize the heavier components and temperature (AlMaamari & Buckley, 2013), water's initial saturation (Jadhunandan & Morrow, 2013).

3.6 Wettability Measurement

Wettability measurement is quite crucial due to its high importance in the design of water flooding. Several different approaches for measuring wettability have been developed, and some of them are explained below.

3.6.1 Contact Angle Measurement

The first approach of determining the wetting state of the fluids is with the help of the measurement of contact angle (Yuan & Lee, 2013). For the measurement of the contact angle, the model environment gets set, the surface of the rock is smoothed after the cut, and then this smoothed surface is exposed to the two different fluids that are immiscible. After the settling of fluids on the surface of the rock, measuring of contact angle is completed through the denser phase, as shown in Figure 3.6 below.

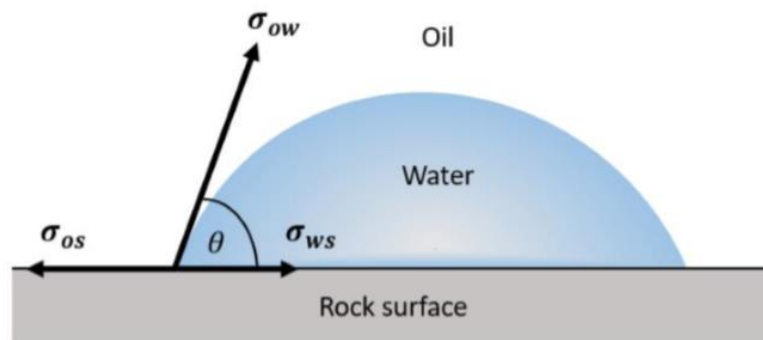


Figure 3.6 Measurement of contact angle (Green and Willhite, 1998)

Young's equation (Equation 3.19) is used to define the static equilibrium in above Figure 3.2. Gibbs stated the thermodynamics basis which was used to develop Young's equation (Letellier et al., 2007).

$$\sigma_{os} = \sigma_{ws} + \sigma_{ow} \cos\theta \quad 3.19$$

Where

- σ_{os} Interfacial tension between oil and solid (mN/m)
- σ_{ws} Interfacial tension between water and solid (mN/m)
- σ_{ow} Interfacial tension between oil and water (mN/m)
- θ Contact angle measured through the denser phase (degree)

The state of wettability can be interpreted through the value of contact angle ranges which is given in Table 3.2 below.

Table 3.2 Wettability states for the range of contact angles

Contact angle, degree	Wettability
0-30	Strongly water wet
30-90	Water wet
90	Neutral wet
90-150	Oil wet
150-180	Strongly oil-wet

This contact angle theory provides the fundamental basis for understanding the concept of wettability, but in this case, the contact angle is measured only on model surfaces that are not true representatives of real reservoir systems. So, it is not realistic to apply this model to the oil-brine systems of the real reservoir rock. This contact angle measurement has another restriction in case of large droplets when the size of droplets is bigger, and these do not get fixed in the pore spaces of diameter of micro or nanometer. Images that are used to measure the contact angle are not applicable as well, even with the usage of micro CT. All of these above-stated problems do make it necessary to consider other methods for the measurement of wettability.

3.6.2 Spontaneous Imbibition

This method is a qualitative method that provides a measurement of relative wettability. Spontaneous Imbibition is quite often used in the industry because the execution and equipment of the process are quite simple (Anderson, 1986).

The process gets started by the placement of the core at initial water saturation in the brine and then letting the core imbibe into the solution of brine freely. During the total test, the volume of oil and rate of oil production is measured. If the total volume of produced oil is high along with the high rate, then the core will be considered as strongly water-wet. If the total volume of oil produced is relatively less at a relatively more minor rate, then the core will be considered relatively less water-wet. On the other hand, if the core cannot imbibe water, it is immersed in residual oil. The assessment will be the same as in the above case, but now only the total volume of produced oil and the rate at which oil is produced will be taken into account. If the rate and total volume are relatively higher, then the core is more water-wet, and if these two factors are relatively lesser, then the core is less water-wet. If any of the two oil or water does not imbibe spontaneously into the core, then it is considered that the core is in a neutral wetting state and has no preference for any of the two fluids.

For the interpretation of the results, a reference should be available which is strongly water-wet due to the fact that the rate of imbibition and wettability depends on several different factors like structure of pores, IFT, core's initial saturation and relative permeability etc. (Denekas et al., 1959, Anderson 1986). In the below Figure 3.7 comparison between the two systems are shown in which one of them is strong and the other is lesser water-wet. Two noticeable differences in curves can be seen in the figure. In the case of strongly water-wet, the gradient of the sample is less steep than the gradient of the reference core, which means that the reference core has a higher rate of imbibition. Moreover, the plateau of the red curve of the sample is lower than the green curve, which signifies the fact that the sample core has more strong water-wet system than the sample core that's why it has the ability to imbibe more fluid. Several different plots like Figure 3.7 can be generated to assess the wettability of sample cores based on the placement and shape of the curve relative to the curve of the reference core.

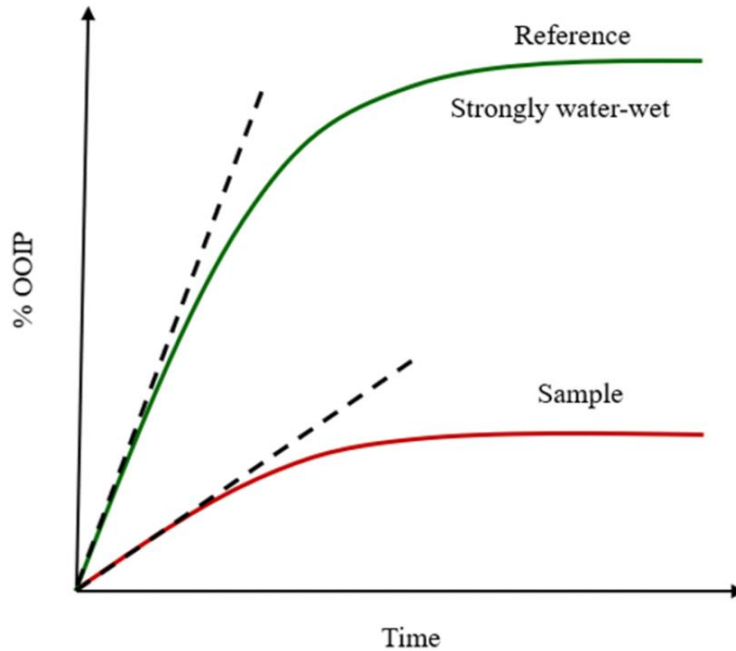


Figure 3.7 Spontaneous imbibition test's illustration. The red curve is showing the sample core, while the green curve is representing the reference core that is strongly water-wet

3.6.3 Amott Method

Two types of imbibition i.e. forced imbibition (FI) and spontaneous imbibition (SI), are applied for measuring the average wettability of core in the Ammot method (Anderson, 1986). These two types of methods are applied for the cancellation of effects of different factors like rock's initial saturation, viscosity, and relative permeability. Therefore, several parameters that can affect the results are removed, and the wettability of the system becomes the governing parameter.

This method has two different parts. In the first part displacing fluid is oil, and in this part, a core that is fully saturated with water is immersed into oil, and that oil imbibe spontaneously into the core displacing the water. The volume of displaced water is measured after the completion of imbibition. Finally, the core is either flooded or centrifuged to saturation of residua water, S_{wr} . The volume of water obtained is also noted, and hence the total volume of water is calculated by adding the volume of water obtained in both steps. The second part of the process is in the same sequence, but the difference is only that the water is used to displace the oil present in the core.

The results of the above experiments will be obtained in the form of Amott wettability indexes i.e., I_O and I_W . I_O is for oil in Equation 3.20, while I_W is for water.

$$I_O = \frac{\Delta S_{OS}}{\Delta S_{OS} + \Delta S_{OF}} \quad 3.20$$

Where

- I_O Amott wettability index to oil
- ΔS_{OS} change of saturation during oil's spontaneous imbibition
- ΔS_{OF} change of saturation during oil's forced imbibition

Whereas the Amott wettability index to water (I_W) is as follows in Equation 3.21,

$$I_W = \frac{\Delta S_{WS}}{\Delta S_{WS} + \Delta S_{WF}} \quad 3.21$$

Where

- I_W Amott wettability index to water
- ΔS_{WS} change of saturation during water's spontaneous imbibition
- ΔS_{WF} change of saturation during water's forced imbibition

I_O values move towards means that core is more oil-wet while the I_W increasing values towards 1 means that the core is more water-wet.

3.6.4 Amott-Harvey method

This method is the modified form of the previously explained Amott method, and the difference between the two processes only lies in the stage of preparation. The stage of preparation can be seen in Figure 3.4 below, indicated by number 1. This shows the oil's forced displacement into the

core and establishment of S_{wr} . In the below Figure 3.8, a plot between capillary pressure (P_c) on the y-axis and saturation of water (S_w) on the x-axis is generated. Moreover, every step in the Amott-Harvey test cycle is explained below with the help of numbers from 1 to 5.

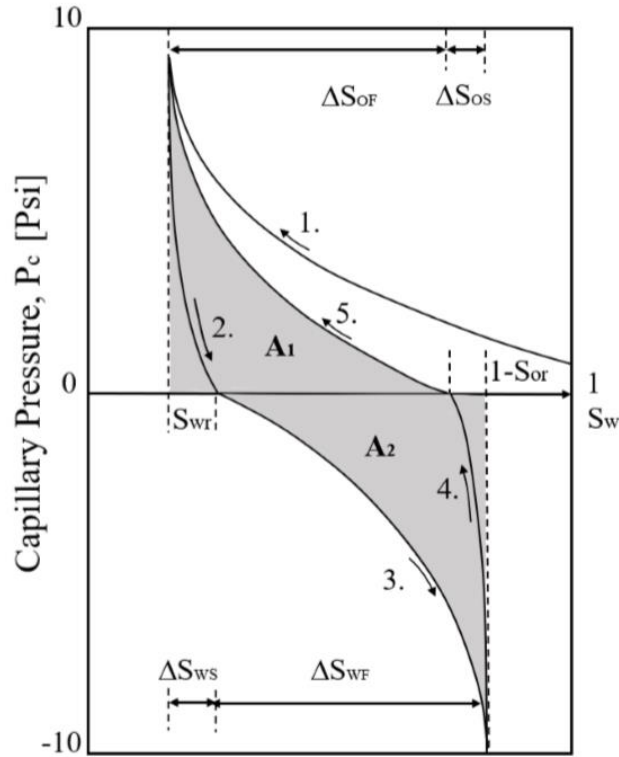


Figure 3.8 Amott and Harvey wettability test's capillary pressure curve (Tina Puntervold, 2008)

Five processes are involved in the above test, which is explained below:

1. For establishing S_{wr} , forced imbibition of oil is done into the core, which is water-saturated.
2. Water's spontaneous imbibition.
3. Water's forced imbibition.
4. Oil's spontaneous imbibition.
5. Oil's forced imbibition.

Relative displacement index (I_{AH}) is the new parameter that is calculated by the difference between the I_w and I_o in Equation 3.22 below.

$$I_{AH} = I_w - I_o \quad 3.22$$

This ratio simply gives the number between -1 and +1. In the case of -1, the core is considered to be oil-wet completely, while +1 indicates that the core is water-wet completely. (Cuiec, 1984) further improved these values and provided a range -0.3 to -0.1 for slightly oil-wet, -0.1 to +0.1 for neutral wet, and = 0.1 to +0.3 for slightly water wet. Ammot Harvey index for different wetting states are given in Table 3.3 below.

Table 3.3 Amott Harvey index for different wetting states

I_{AH}	Wettability State
$-1 \leq I_{AH} \leq -0.3$	Oil-wet
$-0.3 \leq I_{AH} \leq 0.3$	Mixed-wet
$0.3 \leq I_{AH} \leq 1$	Water-wet

3.6.5 Chromatographic Wettability Test

For measuring the carbonate core's wettability, a new method is proposed (Strand et al., 2006). The surface chemistry of minerals is the focus of the chromatographic wettability test, which is unlike both spontaneous imbibition and Amott's method. This method requires a known concentration of SO_4^{-2} and SCN^- in the water, and then the core is flooded with that water. Effluents of flooding are then checked for the concentration of these two anions. The basis of the method is that SO_4^{-2} will get adsorbed on the core, which will be water wet, while SCN^- will not adsorb as seen in Figure 3.9 to 3.12 below.

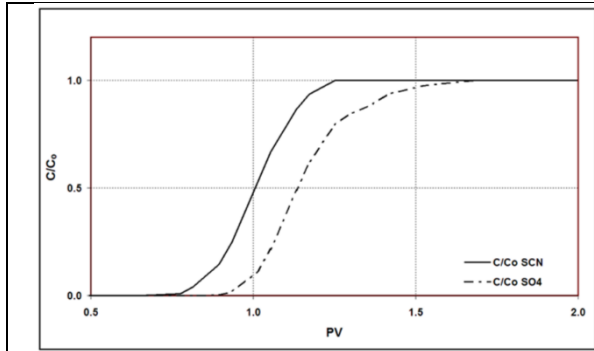


Figure 3.9 Typical chromatography wettability result for a water-wet carbonate core

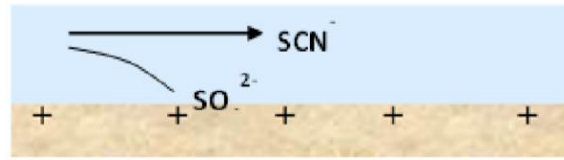


Figure 3.10 Illustration of SCN^- and SO_4^{2-} ions around water-wet carbonate mineral surface.

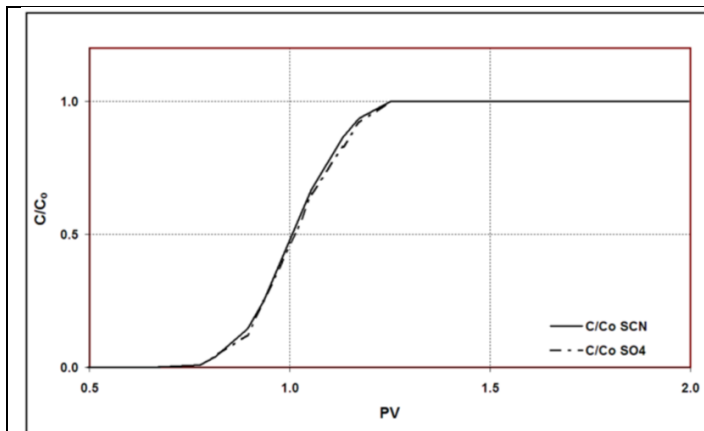


Figure 3.11 Typical chromatography wettability result for an oil-wet carbonate core surface

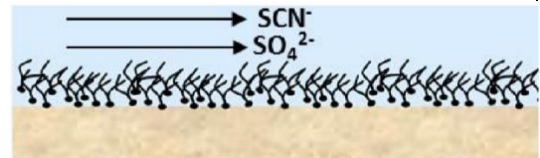


Figure 3.12 Illustration of SCN^- and SO_4^{2-} ions around oil-wet carbonate mineral surface.

Wettability Index (WI) is calculated by using (Equation 3.23) the ratio of SCN^- and SO_4^{2-} curves' area of the sample that was tested.

$$WI = \frac{A_{\text{sample}}}{A_{\text{heptane}}} \quad 3.23$$

Where

WI Wettability index

A_{sample} the area between SO_4^{2-} and SCN^- curves of the sample

A_{heptane} the area between SO_4^{2-} and SCN^- curves completely water-wet reference core containing heptane

In interpretation, Wettability states for the wettability index value are shown in Table 3.4 below.

Table 3.4 Wettability states for the wettability index value

WI_{new} Value	Wettability of system
0	completely oil-wet
0.5	intermediate water-wet
1	completely water-wet

4 Water-Based EOR in Carbonates

4.1 Waterflooding

This is the secondary recovery technique that is used worldwide for slowing down the decline of production by supporting the dropping pressure of the reservoir. Due to its worldwide use, it is possible to study the weaker and stronger sides of this technique. For example, studies of Alvarez and Sawatzky showed that working on waterflooding is not an effective technique in case of heavy oil between heavy oil and water phase there exists a low microscopic displacement efficiency (Alvarez & Sawatzky, 2013). Whereas another study made by Wade based on 53 waterflooding technique cases shows that, off the total pore volume, the waterflooding made an average oil recovery of approximately 23.3 percent while the original average primary recovery was only 9.4 percent (Wade, 1971). These results of Wade show that waterflooding is quite effective in increasing the production of reservoirs. Along with the advantage of the high recovery, this technique also has several drawbacks like problems of sand production, water compatibilities issues, corrosion control, and issues related to scaling, so all of these problems will be kept in mind before designing the water for waterflooding technique.

Furthermore, the composition of injection water has been researched extensively after seeing the fact that all injected water has not shown the same oil displacement results. So different water injection has been studied to understand their displacement efficiency. Oil displacement in carbonates has been done with sea water which has shown relatively good results. Seawater acts as a natural enhancer of displacement, so extensive studies have been carried related to its composition and other properties.

4.2 Wettability Alteration in Carbonate by Modifying the Ionic Composition of Water

Seawater enhances the displacement of oil, so studies have been done about the mechanism that made this water a good injection water for displacement in carbonates. Seawater does not have

any enhancement in its macroscopic displacement efficiency on its own, so the studies' main focus has been towards its properties that affect its ability of macroscopic displacement efficiency like oil-brine-rock system's wettability. By changing the ionic composition of flooding, water enhances its wetting state in the porous medium, thus increasing the flooding efficiencies (S. Strand et al., 2006; Zhang & Austad, 2006; Zhang et al., 2007a). It has been discovered that oil displacement will be improved by seawater in fractured reservoirs made of chalk by altering the wettability (Strand et al., 2008).

In Figure 4.1 below, Strand et al. experimented with two chalk cores that were restored equally at the temperature of 120 °C. This experiment has sequential processes of spontaneous imbibition followed by viscous flooding of these two chalk cores. The cores were named C#6 and C#7. The first core C#6 was imbibed spontaneously with FW initially, and as a result recovery of 12 percent of OOIP has been made. The SI brine of the core is changed to SW next, and as a result, an extra 18 percent of the oil of OOIP has been recovered. This improvement in recovery shows that SW is a valid modifier of wettability, and it acts as Smart water at 120 °C for chalk reservoirs.

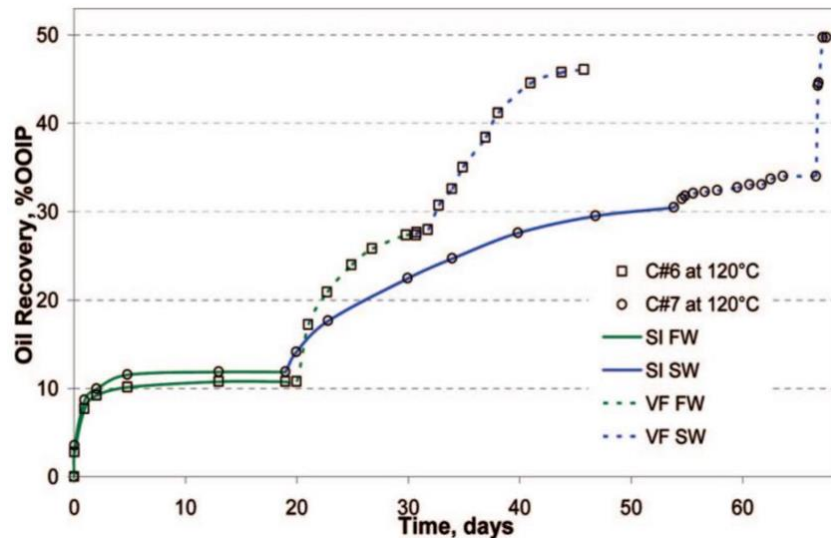


Figure 4.1 Recovery of oil made at 120 °C by spontaneous imbibition and forced displacement successively (Strand et al., 2008)

Another study has been made by Zhang, 2006 about the effects of different injection brines on the displacement of efficiency on the chalk cores, which were equally restored as shown in Figure 4.2 below. In this study, FW with no sulfate is imbibed spontaneously into the core, and as a result, an

18 percent recovery of OOIP has been made. To see the effects of SW, instead of FW, spontaneous imbibition of SW has been made into chalk core, and as a result, 38 percent of OOIP recovery has been made, and this extra 20 percent recovery shows that SW modifies the wettability of chalk cores at 90 °C and acts as Smart water.

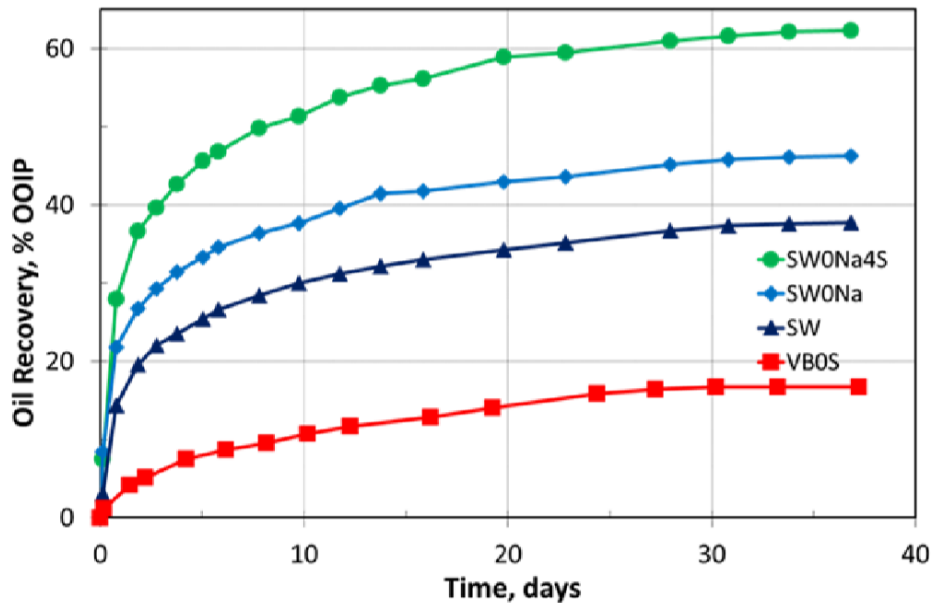


Figure 4.2 Tests of SI at 90 °C on chalk cores restored equally. Modified SW as Smart Water imbibing brines (Fathi et al., 2011)

4.2.1 Na⁺ Effect

Zhang, 2006 made another study about the concentration of Na⁺ in the injection brine of SW. The concentration of sodium ions was removed from SW, and core at 90 °C was imbibed spontaneously with that SW and an extra recovery of 10 percent of oil of OOIP has been recovered, which shows that removal of sodium ions enhances the ability of SW to displace oil by altering the wettability of SW at 90 °C.

4.2.2 SO₄²⁻ Effect

In the same study explained above by Zhang, the effect of the concentration of SO₄²⁻ has been studied as well. Zhang, along with the removal of sodium ions he spiked the concentration of

sulfate ions four times in the SW. After that, this modified SW with no sodium ions and 4 times sulfate ions concentration of the original SW is imbibed spontaneously with and this made an extra recovery of 18 percent than the SW with no sodium ions (Figure 4.2). Total oil recovery has moved to 62 percent of OOIP, which shows that sulfate ions concentration is significant for the alteration of wettability; thus, increasing the concentration of these ions increases the wettability alteration and ultimately the recovery of SW at 90 °C.

The concentration of sulfate ions has been studied separately by Zhang as well as shown in Figure 4.3 below. He confirms the fact that increasing the concentration of sulfate ions enhances wettability and increases oil recovery.

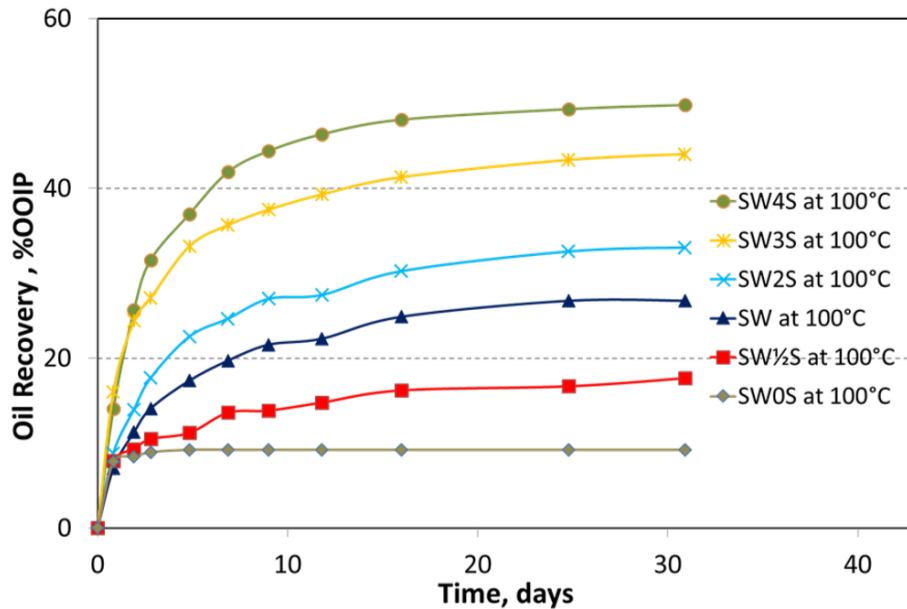


Figure 4.3 Test results of SI at 100 °C on chalk cores equally restored (Zhang, 2006)

4.2.3 Ca²⁺ Effect

The effect of variable concentration of Ca²⁺ on the recovery of oil has been studied by Zhang as well. He uses five different brines for imbibition with different concentrations of calcium ions at 70 °C. These brines were prepared on the basis of SW. Figure 4.4 shows that the increasing concentration of calcium ions increases the SW potential of altering the wettability and thus increases the oil displacement with better results of recovery.

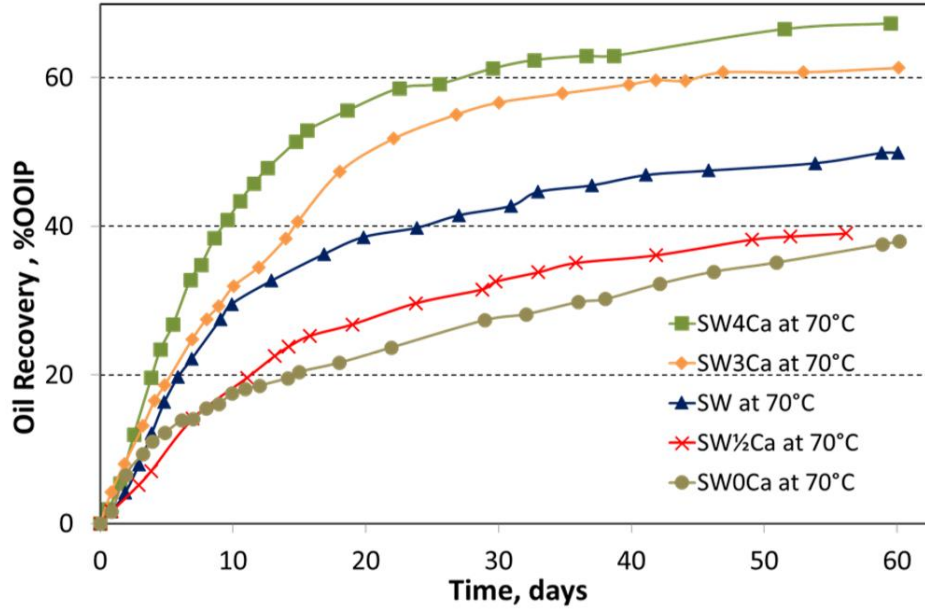


Figure 4.4 Test results of SI at 70 °C on chalk cores equally restored. Ca^{2+} concentration increase in SW imbibing brine (Zhang, 2006)

4.2.4 Mg^{+2} Effect

Zhang studied another important cation, Mg^{+2} , for the alteration of the wettability in carbonates (Zhang et al., 2007b). Chalk cores that were equally restored were tested SI with different brines in the study, and the results are given in Figure 4.5 below. Imbibition of core CM-1 was done with SWO brine having the composition of 1 time of SO_4^{-2} , no Mg^{+2} , and no Ca^{+2} at the temperature of 100 °C. As a result, 12 percent of OOIP has been recovered. Then on day 43, a number of magnesium ions were added to SI brine, and as a result, an extra 20 percent of OOIP has been recovered compared to the SWO brine. These results indicate that at 100 °C in chalk cores, magnesium has altering properties for wettability.

On the same day, the interesting effect of magnesium ions was shown by Zhang as well. At the temperature of 100 °C, results of SI were similar for both of the cores, i.e., CM-2 and CM-4, and the imbibition of these cores was done with SWO-OS bring having a composition of no magnesium, calcium, or sulfate ions and SWO-4S brine having the composition of no magnesium or calcium ions but four times of sulfate ions respectively. The results of these imbibitions made the recovery of around 12 percent of OOIP. These results indicate that if calcium and magnesium

are absent, then sulfate ions lose their power of altering the wettability of chalk cores at the temperature of 100 °C. Later in the same experiment, at day 53, Zhang added SW amount of magnesium in both the imbibing fluids of SWO-OS and SWO-4S and obtained the recovery of an extra 10 percent and 30 percent of OOIP, respectively. The results show that magnesium does have some potential for altering the wettability, but the results were still less than the brines having 4 times of sulfate ions in them as seen in Figure 4.5 below.

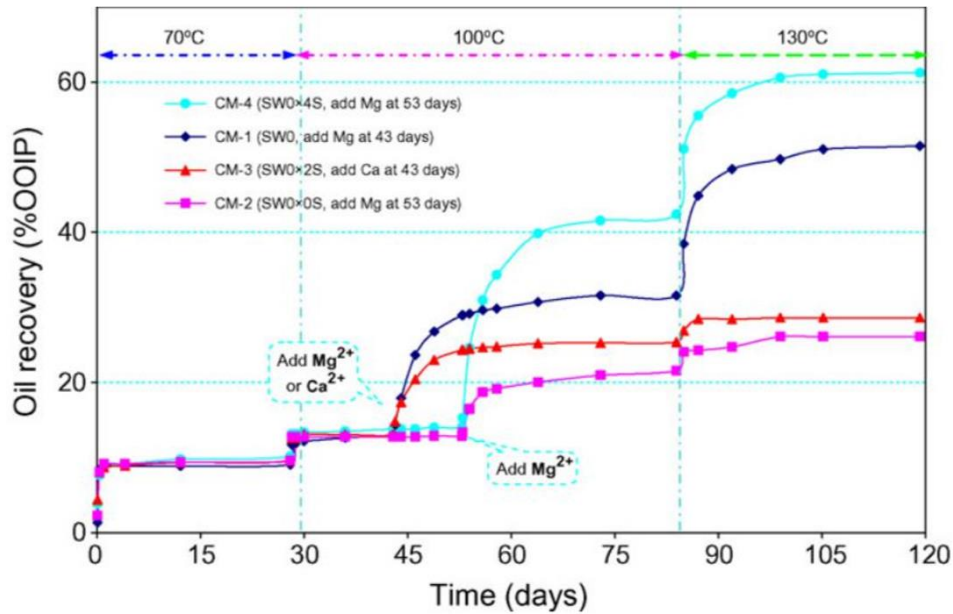


Figure 4.5 Tests of SI tests done at different temperature of 70 °C, 100 °C, and 130 °C with and without concentration of Calcium and Magnesium ions (Austad et al., 2007)

4.2.5 Temperature Effect

Temperature effect on the alteration of wettability has been studied by Strand et al. (Strand et al., 2008). He sequentially spontaneous imbibe and viscous the cores of chalk with seawater. As shown in Figures 4.6 and 4.7 below, the capability of seawater to modify wettability at the temperature of 90 °C with SI is very negligible, with only increasing the oil recovery by 2 percent of OOIP.

Although, at the temperature of 120 °C, the power of seawater increases for altering the wettability for both the viscous flooding and spontaneous imbibition as shown in Figure 4.7 below. Core C#6 was imbibed with formation water at 120 °C, and recovery was increased to 12 percent of OOIP,

and then the imbibing brine was changed into SW from FW, and the total recovery made was 30 percent of OOIP. These results show that without changing any other properties like mobility ratio etc, only the change of water from formation water to seawater also significantly impacts the recovery (18 percent of extra recovery). Hence, seawater has the capabilities of altering the wettability of chalk cores, and this effect is directly related to the temperature, and with an increase in the temperature, the wettability got changed as well (Strand et al., 2008).

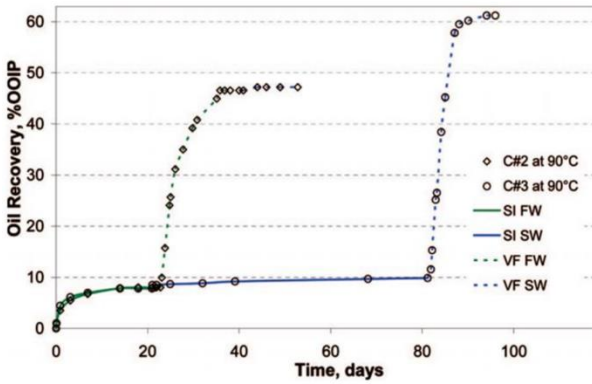


Figure 4.6 Oil recovery at 90 °C by successive spontaneous imbibition and forced displacement

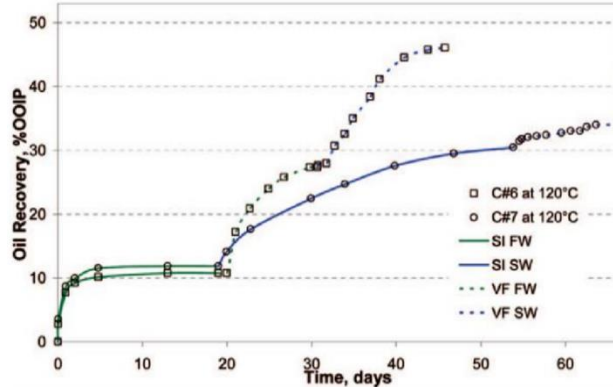


Figure 4.7 Oil recovery at 120 °C by successive spontaneous imbibition and forced displacement

4.3 Smart Water

The composition of optimized Smart Water has been studied previously and seen the behavior of seawater to act as Smart Water at high temperatures. But at the lower temperatures, the seawater's efficiency could be improved by altering the composition as shown in Figure 4.8.

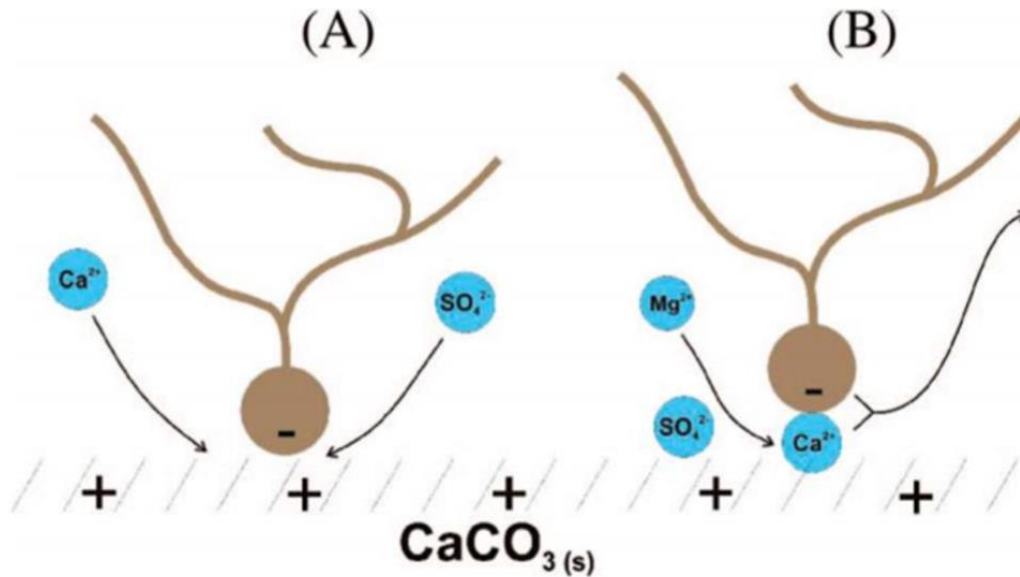


Figure 4.8 Suggested wettability alteration mechanism with seawater. Figure from smart water group at University of Stavanger

Above Figure 4.8 shows the suggested alteration mechanism of wettability in chalk by seawater (A) when Ca^{+2} and SO_4^{-2} are active (B) when Mg^{+2} and SO_4^{-2} are active at high temperatures (Torrijos et al., 2019)

Smart Water's design for altering the wettability in carbonates has relied roughly on the following properties:

- NaCl's reduced concentration.
- SO_4^{-2} , Ca^{+2} , and Mg^{+2} concentration in optimum amount.
- The optimum concentration of ions will be considered that amount that has a high recovery rate and no precipitation of salt at favorable temperature.
- The Mg^{+2} concentration cannot be overlooked in Smart Water and should be considered especially for dolomite reservoir's design for Smart Water.

5 Experimental Work

5.1 Materials

5.1.1 Core Material

In order to resemble the biogenic chalk reservoirs found at the Norwegian continental shelf, among them Ekofisk and Valhall, the outcrop Stevns Klint chalk close to København were used as an analog to the natural reservoir rock. The carbonates have the same age as the upper Tor and lower Ekofisk formation and are reported to be 98-99 % pure biogenic chalk (Frykman, 2001). Cores from Stevns Klint outcrop chalk in Sjælland, Denmark, have been used in this research study. All of three cores were drilled in the same rock block in a similar direction. After that, cores have been shaved and then cut in the wanted dimensions. The three cores studied, i.e., Core#1, Core#2 and Core#3 have been presented in Table 5.1 below.

Table 5.1 Measured Properties of Three Studied Cores

Core Name	Length (cm)	Diameter (cm)	Bulk Volume (cm³)	Pore Volume (ml)	Porosity (fraction)	k (mD)	Swi (%)	OOIP (ml)
Core #1	6.713	3.81	76.53	37.97	0.4961	-	10	55
Core #2	7.05	3.81	80.46	39.59	0.4921	3.16	10	65.8
Core #3	6.86	3.81	78.38	37.77	0.4818	-	10	53.8

5.1.2 Selection of Crude Oil

A general description of the process of modifying crude oil to different AN is given here. The crude oils that come directly from reservoirs have very high AN, and it is, therefore, necessary to modify the crude oil to AN-values. The oil was already prepared in the lab according to the following procedure.

5.1.2.1 RES-40 Preparation

Res-40 that is used as base oil, was prepared by the dilution of Heidrun crude oil with the help of n-heptane, and the volume in which dilution occurs was 60:40, respectively. Surface-active components were removed from Res-40 with the help of silica gel treatment. After this removal of surface-active components, the base oil was centrifuged and then filtered through a filter of 0.5 μm Millipore.

5.1.2.2 RES-40-Zero Preparation

After all of these treatments the due to low surface-active components in the base oil the resultant treated oil is known as Res-40-zero. The RES-40-zero has $\text{AN} = 0$ and is made with RES-40 as the basis oil. The preparation of the oil begins by adding 20 wt% silica gel to the RES-40 oil, followed by 1 week of stirring at room temperature. The role of the silica gel is to extract the polar oil components out of the oil, hence reducing the acid number of the oil. Then an additional 20 wt% silica gel is added to the oil and put on stirring for an additional week. After a total of two weeks of stirring, precipitates have formed, which are due to the adsorption of polar oil components into the silica gel. Next, the oil is centrifuged in order to separate the silica gel from the oil phase. Afterward, the oil was filtered with a 5 μm millipore filter and stored in a flask.

5.1.2.3 Oil-A Preparation

Oil A which has base number (BN) = 0.31 mg KOH/g and acid number (AN) = 0.53 mg KOH/g was obtained by mixing Res-40-zero with Res-40. Oil A was then used throughout the whole experiment. $\text{AN}_{\text{Target}}$ was calculated through Equation 5.1 and measured properties of oil are given in Table 5.2 below.

$$\text{AN}_{\text{Target}} = \text{AN}_{\text{Res-40}} \frac{V_{\text{Res-40}}}{V_{\text{Res-40}} + V_{\text{Res-40-zero}}} + \text{AN}_{\text{Res-40-zero}} \frac{V_{\text{Res-40-zero}}}{V_{\text{Res-40}} + V_{\text{Res-40-zero}}} \quad 5.1$$

Table 5.2 Measured Properties of Oil

Oil Name	Density (g/cm ³)	AN (mgKOH/g oil)	BN (mgKOH/g oil)	Viscosity (cP)
Res-40	0.82	1.85	0.67	2.7
Res-40-zero	0.81	0.01	0.03	2.4
Oil-A	0.81	0.53	0.31	2.5

5.1.3 Compounds

Two different types of compounds were used in this research to produce different ions used for the preparation of Smart Water. Following two compounds, i.e., Calcium sulfate and Magnesium Chloride, were used.

5.1.3.1 Calcium Sulphate (CaSO₄)

Calcium sulfate is an inorganic chemical compound also known as gypsum in its hydrous form. Another hydrous form of calcium sulfate is known as Plater of Paris, while the anhydrous form is called anhydrite. There are several uses of calcium sulfate in the industry, starting from the production of Plaster of Paris and stucco.

5.1.3.2 Magnesium Chloride (MgCl₂)

Magnesium Chloride is a chemical compound that has several hydrates MgCl₂(H₂O)_x. Anhydrous MgCl₂ has a high percentage of magnesium by mass, i.e., 25.5 percent. They are highly soluble in water because they are typical ionic halides. Sea water or brine can be used to extract hydrated form of Magnesium Chloride. This compound has various applications in dust and erosion control, catalyst support, control of ice, nutrition and medicine, gardening and horticulture, etc.

5.1.4 Brines

5.1.4.1 Preparation of Brines

Synthetic preparation of all the brines used in this study occurred in the laboratory, and the composition of all these synthetically prepared brines has been given in Table 5.3 below. For avoiding precipitation, different salts like SO₄⁻², Cl⁻ and CO₃⁻² were dissolved in de-ionized water

separately. After the dissolution of all salts, the volumetric flask was filled up to meniscus and put on stirring at 23 °C for 24 hours. Visual assurances of the mixtures have been made to confirm the negligible precipitation of calcium (anhydrite). After this confirmation, individual brines have been obtained by combining different mixtures. Finally, the filtration of brines was carried out through a filter of size 0.22 µm Millipore.

5.1.4.2 Valhall Formation Brine FW (VB0S)

Water saturation in the chalk cores were initially established with a brine termed as VB0S. This brine has a composition similar to the formation water in the chalk formation Valhall, situated in the southern side of North Sea, but only difference is that it does not contain SO_4^{2-} . The removal of SO_4^{2-} in establishment of initial saturation is important because sulfates can render the the core water-wet (Punternold et al., 2007). This fluid was used for spontaneous imbibition tests as imbibing fluid for Core#1 shown in Table 5.3.

5.1.4.3 Smart Water

Two different types of Smart Water were prepared by using CaSO_4 and MgCl_2 in different proportions.

5.1.4.3.1 Smart Water-1 (SmW-1)

This Smart Water was prepared by using the concentration CaSO_4 (20mM) and MgCl_2 (20mM) in 1:1. This Smart Water-1 was used as imbibing fluid for the spontaneous imbibition test of Core 1 and Core 2.

5.1.4.3.2 Smart Water-2 (SmW-2)

This Smart Water was prepared by using the concentration CaSO_4 (20mM) and MgCl_2 (40mM) in 1:2. This Smart Water-2 was used as imbibing fluid for the spontaneous imbibition test of Core 3.

Table 5.3 Brine Compositions and Properties

Ions	FW (mM)	SW (mM)	SmW-1 (mM)	SmW-2 (mM)
HCO ₃ ⁻	9	2	0	0
Cl ⁻	1066	525	20	40
SO ₄ ⁻²	0	24	20	20
Mg ⁺²	8	45	20	40
Ca ⁺²	29	13	20	20
Na ⁺	997	450	0	0
K ⁺	5	10	0	0
Density at 20 °C (g/cm ³)	1.041	1.022	1.0019	1.0035
TDS (g/l)	62.83	33.39	6.789	10.855
Ca ⁺² /SO ₄ ²⁻	N/A	0.540	1	1
Mg ⁺² / Cl ⁻	0.007	0.085	1	1
CaSO ₄ / MgCl ₂	0.027	0.064	1	0.5

5.2 Analysis

During the experimental work, several analyses were carried out. Hence a brief introduction of the equipment that was used for each analysis is given in this section.

5.2.1 pH Measurement

To measure the pH of the brine of CaSO₄ and MgCl₂ with and without NaHCO₃ and brine of CaCl₂ and NaSO₄, a pH meter known as Seven Compact from Mettler Toledo was used. The pH meter has a calibration program for quality assurance. Thus, each time the instrument was used, it was calibrated with buffer solutions of pH = 4, 7, and 10.

5.2.2 PHREEQC

In order to look for the precipitation in the simulation, PHREEQC was used to establish the CaSO₄ precipitation. Precipitation of calcium was observed for two different solutions i.e. CaSO₄ with MgCl₂ solution and NaSO₄ with CaCl₂.

5.2.3 Temperature stability of brine

5.2.3.1 Bulk Test Analyses

The first type of brine was prepared by CaSO_4 and MgCl_2 in four different quantities or volumes, i.e., 10 mM, 15 mM, 20 mM, and 25 mM. Another type of brine was prepared by adding 2 mM sodium bicarbonate (NaHCO_3) in 10 mM, 15 mM, 20 mM, and 25 mM solutions of CaSO_4 and MgCl_2 . The third brine was prepared by mixing Na_2SO_4 and CaCl_2 in three different quantities that were 10mM, 15 mM, and 20mM. All of these prepared brines were left overnight at the temperature of 130 °C. Then the vials were placed in a centrifuge for 5 minutes, and precipitation was seen.

5.2.3.2 Ion Chromatography Analyses of Brines

Ion chromatography of Smart Water containing CaSO_4 and MgCl_2 was done at room temperature and at 130 °C. Ion chromatography of Smart Water containing CaSO_4 and MgCl_2 along with 2mM NaHCO_3 was done at room temperature and at 130 °C as well.

5.3 Methodology

In this section, the methodology of the experimental part is presented. The Smart Water group at UIS has worked with Stevns Klint chalk for over 20 years and has therefore established a set of steps on how the cores must be prepared to best represent a reservoir chalk core. A general methodology of how each core was prepared is given, along with a description of how the acid flooding, spontaneous imbibition and forced imbibition were conducted.

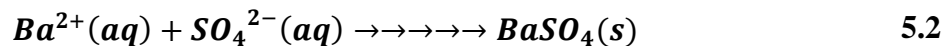
5.3.1 Core Cleaning

Since the Stevns Klint area is situated close to the sea, there is a high possibility that the cores contain SO_4^{2-} due to contact with SW. Therefore, all chalk cores, regardless of the type of experiment, had to be cleaned with DI water. As previously discussed, even a small concentration

of SO_4^{2-} present in the core can have a strong influence on the initial wetting since the sulfate hinders the organic oil components from adsorbing onto the mineral surface (Punternvold et al., 2007). It also serves to get rid of salts that are easily dissolvable.

The cleaning process was done as proposed by Punternvold et al., 2007, where it is suggested to flush the core with at least 4 PVs of a brine free of SO_4^{2-} and without negatively charged ions. Therefore all cores were cleaned by flooding over 4 PVs with DI-water at a rate of 0.1 ml/min at room temperature. As all the chalk cores were relatively fragile, the confining pressure was set at 20 bars during flooding. Batch tests of the effluent were then taken and further mixed with Ba^{2+} to check if any precipitation of $\text{BaSO}_4(\text{s})$ took place. Consequently, if there are SO_4^{2-} , reaction (5.2) will take place, and the water will no longer be blank but rather look cloud

Punternvold prepared a procedure for cleaning cores, and that method was used in this research for cleaning cores (Punternvold et al., 2007). At room temperature, de-ionized water of 5 PV was used to flood cores at a rate of 0.1 ml/min. Qualitative tests were conducted on the collected effluent samples. Samples were qualitatively analyzed to see the presence of SO_4^{2-} . During qualitative tests, BaCl_2 was added to the effluent samples to see the precipitation of BaSO_4 . The reaction is given in Equation 5.2 below.



5.3.2 Porosity Measurement

The bulk volume was found by measuring the length and diameter of the cores. Subsequently, the dry weight, W_{dry} , and the saturated weight, W_{sat} were measured. To ensure that the cores were Fully saturated, they were put in a vacuum before being saturated to remove air. Since the density of the DI-water, ρ_w was close to 1.00 g/cm³, V_p was found by taking the Difference between W_{sat} and W_{dry} .

At a temperature of 90 °C, cores were dried to constant weight. W_{dry} was measured by weighing these dried cores. After this, the saturation of these dried cores with de-ionized water in the vacuum cell was done, and the weight of these cores was indicated by $W_{saturated}$. Both of these weights in

grams, the density of de-ionized water at 20 °C (ρ_{DI}) in g/cm³, and a bulk volume of core (V_{bulk}) in cm³ were used to calculate porosity (φ) in fraction as shown in Equation 5.3 below.

$$\varphi = \frac{\frac{W_{saturated}}{\rho_{DI}}}{V_{bulk}} \quad 5.3$$

Where,

φ	Core's porosity in fraction
$W_{saturated}$	Saturated core's weight in grams
ρ_{DI}	De-ionized water's density at 20 °C in g/cm ³
V_{bulk}	Core's bulk volume in cm ³

5.3.3 Permeability Measurement

Flooding setup was arranged at room temperature to measure the permeability with a back pressure of 8 bar to confirm the control over the pressure difference (ΔP) between outlet and inlet. Each of the three cores was then flooded with de-ionized water at different flow rates of 0.05, 0.1, and 0.15 ml/min. Pressure differences obtained during different flow rates were recorded, and below, Equation 5.4 was used to calculate the permeability (k) in mD.

$$k = \frac{Q\mu L}{\Delta P A} \quad 5.4$$

Where:

k	Permeability of rock in Darcy
Q	Flow rate in ml/s
μ	Flooding fluid's viscosity in cP,
L	Core's length in cm

A Cross-sectional flow area in cm^2

ΔP Inlet and outlet's pressure difference in atm

After the measurement of permeability, the cores were then dried to constant weight at $90\text{ }^\circ\text{C}$.

5.3.4 Core Restoration for Spontaneous Imbibition Experiments

Before the spontaneous imbibition (SI), the cores went through a restoration process to establish the formation of water and oil saturation. The cores were saturated with $S_{wi}= 10\%$ FW and $S_{oi}= 90\%$ with oil A of AN = 0.50 mg KOH/g.

5.3.4.1 Establishing Initial Water Saturation

After measuring the dry weight of the core, the weight that was targeted with the saturation of water at 100 percent was calculated by using Equation 5.5 given below. The core, after drying and cleaning were fully saturated with Valhall brine, i.e., 10 times diluted (d10VB0S) in a vacuum cell (Springer et al. 2003). For the absorption of water from the core, the desiccator with silica gel at the bottom was used. The weight of the core was measured in intervals until the target weight had been reached. After the targeted weight was achieved, the 10 percent initial water saturation with VB0S was established certainly. Subsequently, this core was securely placed in the container which was sealed and left to rest for 3 days to allow all the introduced brine to diffuse all around the core.

$$W_{target} = W_{dry} + 0.1xPVx\rho_{VB0S} \quad 5.5$$

Where:

W_{dry} , Dry core's weight in grams

PV , Pore Volume in ml

ρ_{VB0S} , VB0S Brine's density at 1.0224 g/cm^3

5.3.4.2 Establishing Oil Saturation

Core with initial saturation of 10 percent was placed in the heating system in Hassler core holder. For providing an air-free oil saturation to the core, all of the air was vacuumed from air spaces before injection of oil. After complete removal of air, Oil A (1 PV) was injected at a rate of 0.5 ml/min from both sides of the core. Then Oil A (2 PV) was injected at the rate of 0.2 ml/min in the direction from right to left and then vice versa. Finally, the core was weighed to confirm the 90 percent oil saturation of the core. Set-up for oil saturation establishment is shown in Figure 5.1 below.

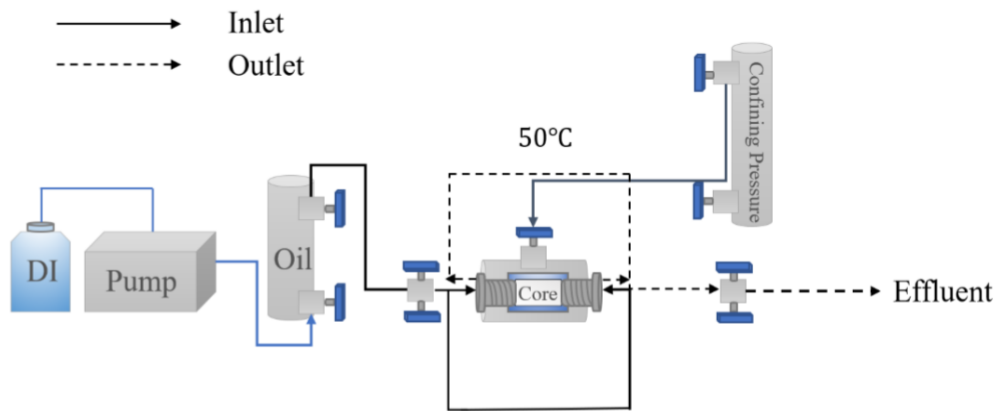


Figure 5.1 Set-up for oil saturation establishment (Lindanger, 2019)

5.3.4.3 Ageing

Cores that were saturated with 10 percent of water and 90 percent of the oil were protected by wrapping in Polytetrafluoroethylene film tape to ensure no loss of constituents. Then these wrapped cores were left for the purpose of aging for 14 days at 90 °C in a cell that was filled with Oil A.

5.3.5 Oil Recovery by Spontaneous Imbibition Test

After ageing, the cores were then placed in imbibing fluid-filled imbibition cell which was connected to imbibing fluid-filled piston cell to provide pressure support; the system was pressurized at 10 bar as well. This pressure of 10 bar was necessary for fluids of imbibition cell

and core to stay in liquid phase at a high temperature of 130 °C. The oil which was produced were collected and noted for the calculation of Original Oil in Place (%OOIP). Set-up used for Spontaneous Imbibition Test is shown in Figure 5.2 below.

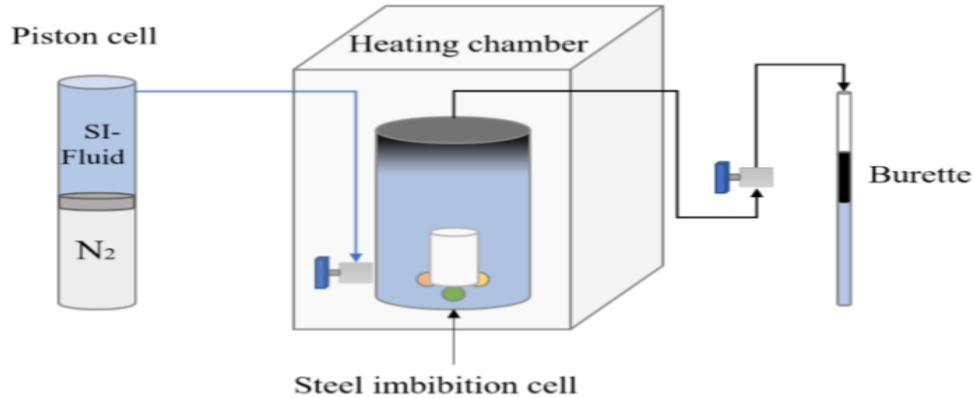


Figure 5.2 Set-up used for Spontaneous Imbibition Test (Lindanger, 2019)

5.3.6 Selection of Optimum Brine with respect to Precipitation

Three different types of brines were prepared to look for the optimum brine to use in the study, which has no or relatively less precipitation. As precipitation effects the recovery of the oil so it was in the best interest to look for the brine that was producing less or no precipitation at all.

6 Results

6.1 pH Measurement

For measuring the pH of the brines of CaSO₄ and MgCl₂ with and without NaHCO₃ and brine of CaCl₂ and NaSO₄, a pH meter known as Seven Compact from Mettler Toledo was used. This pH meter has a calibration program for the assurance of quality. The results of pH are represented in Table 6.1 below.

Table 6.1 pH of the brines of CaSO₄ and MgCl₂ with and without NaHCO₃ and brine of CaCl₂ and NaSO₄

CaSO ₄ and MgCl ₂ (with NaHCO ₃)		CaSO ₄ and MgCl ₂ (without NaHCO ₃)	
Solution	pH	Solution	pH
10 mM	8.84	10 mM	7.06
15 mM	8.64	15 mM	7.13
20 mM	8.96	20 mM	7.16
25 mM	8.30	25 mM	7.19
CaCl₂ and NaSO₄			
	Solution	pH	
	10 mM	8.67	
	15 mM	8.01	
	20 mM	7.57	
	25 mM	7.11	

6.2 PHREEQC

In order to look for the precipitation in the simulation, PHREEQC was used to establish the CaSO₄ precipitation. Precipitation of calcium was observed for two different solutions i.e. CaSO₄ and MgCl₂ solution and NaSO₄ and CaCl₂. Results can be seen in Figure 6.1 below. The solution of CaSO₄ and MgCl₂ shows relatively low precipitation of calcium at 130 °C.

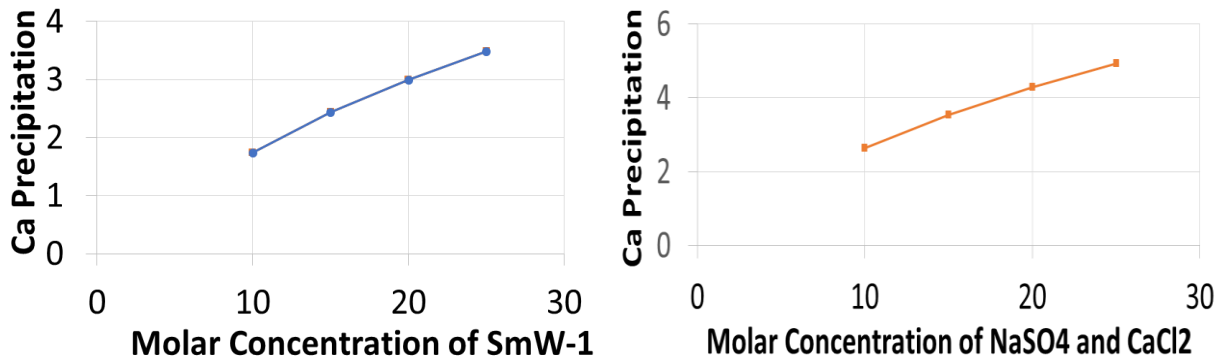


Figure 6.1 Comparison of Ca precipitation of CaSO_4 with MgCl_2 (1:1) (left) and NaSO_4 with CaCl_2 (1:1) (right) solutions at $130\text{ }^\circ\text{C}$

The solution of CaSO_4 and MgCl_2 shows relatively low precipitation of calcium than NaSO_4 and CaCl_2 at $130\text{ }^\circ\text{C}$.

The ratio of CaSO_4 and MgCl_2 was changed from 1:1 to 1:2 to look for a change in results which further decreases the concentration of precipitation of calcium at $130\text{ }^\circ\text{C}$ as shown in Figure 6.2 below.

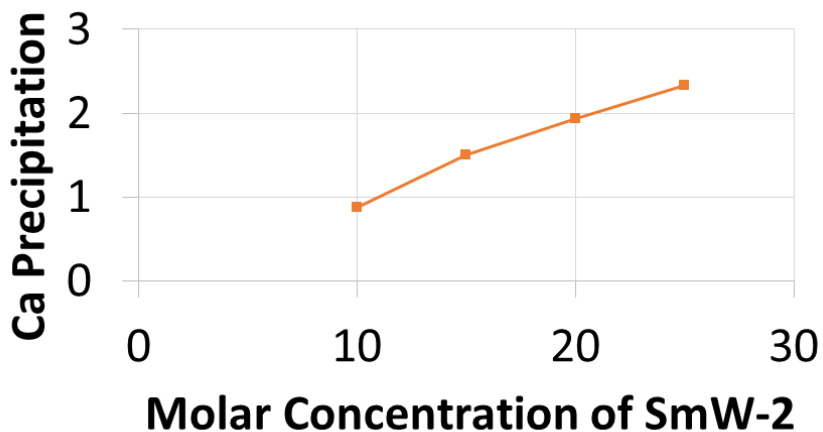


Figure 6.2 Ca precipitation of CaSO_4 and MgCl_2 (1:2) solution at $130\text{ }^\circ\text{C}$

A further change in the ratio of CaSO_4 and MgCl_2 from 1:2 to 1:3 further decreases the concentration of precipitation of calcium at $130\text{ }^\circ\text{C}$, as shown in Figure 6.3 below.

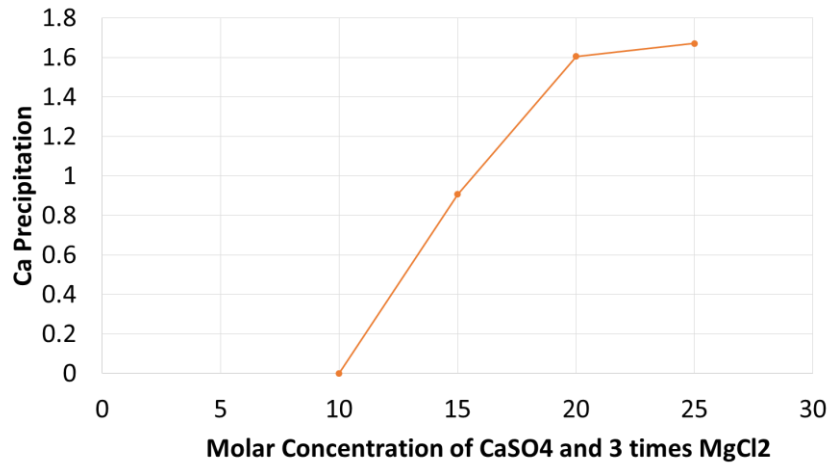


Figure 6.3 Ca precipitation of CaSO₄ and MgCl₂(1:3) solution at 130 °C

6.3 Temperature stability of Brine

6.3.1 Bulk test analyses

The first brine prepared was a mixture of CaSO₄ and MgCl₂ in four different quantities or volumes, i.e., 10 mM, 15 mM, 20 mM, and 25 mM (Figure 6.4). All of these four prepared solutions were left overnight at the temperature of 130 °C. Then the vials were placed in a centrifuge for 5 minutes, and precipitation was seen. The 10 mM solution shows no precipitation, 15 mM solution had less precipitation, 20 mM solution had relatively higher precipitation, while the 25 mM solution had the maximum amount of precipitation. Precipitation increases due to an increase in molarity of CaSO₄.



Figure 6.4 Vials containing different concentration solutions of CaSO_4 and MgCl_2

The second type of brine was prepared by adding 2 mM sodium bicarbonate (NaHCO_3) in 10 mM, 15 mM, 20 mM and 25 mM solutions of CaSO_4 and MgCl_2 (Figure 6.5). After addition of sodium bicarbonate in all these solutions the resultant solution was left overnight at 130°C and then placed in centrifuge for 5 minutes to look for precipitation. The result of these solutions were almost same as the previous solutions that were without sodium bicarbonate, so results indicates that sodium bicarbonate have no impact on the precipitation.

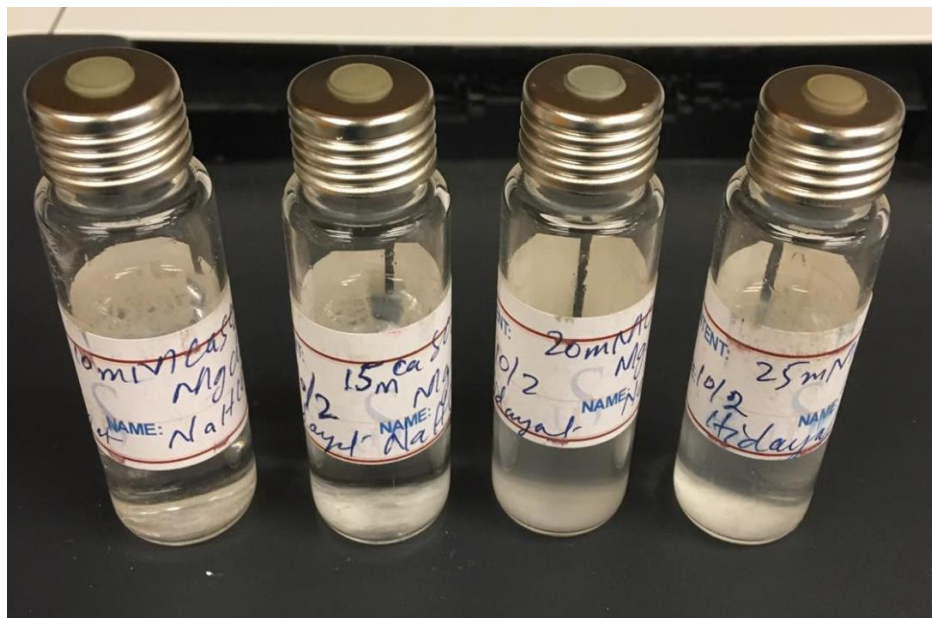


Figure 6.5 Vials containing solutions of CaSO_4 and MgCl_2 (having different concentration of NaHCO_3)

The third brine was prepared by mixing NaSO_4 and CaCl_2 in three different quantities that were 10mM, 15 mM, and 20mM (Figure 6.6). These solutions were run through the same process of leaving overnight at 130 °C and then placed in a centrifuge for 5 minutes. The results were not good in this case as well because there were signs of precipitation even in the 10 mM solution.



Figure 6.6 Vials containing different concentration solutions of NaSO_4 and CaCl_2

The best brine which was selected was 10 mM solution of CaSO_4 and MgCl_2 , which had no precipitation at all.

6.3.2 Chemical analyses of brines using Ion Chromatography

Ion chromatography of Smart Water containing CaSO_4 and MgCl_2 was done at room temperature and at 130 °C. The results of ion chromatography can be seen in Table 6.2 below.

Table 6.2 Ion Chromatography results of brines with different molar concentration at room temperature and at 130 °C

Smart Water (CaSO ₄ and MgCl ₂)				
	At room temperature		After 130 °C	
Molarity	Calcium Ions	Sulphate Ions	Calcium Ions	Sulphate Ions
10 mM	7.9	9.8	8.2	9.8
15 mM	15	15	13.7	13.1
20mM	20.3	20.1	16.7	14.6
25 mM	63.8	54	16.4	16.7

The results show a high concentration of calcium in 10mM solution at 130 °C than room temperature and approximately the same sulfate ions for both while trend is reverse for the concentration of calcium and sulfate ions in 15mM and 20 mM solution as shown in Figure 6.7 and 6.8 below. Hence the values for the 25 mM solution of CaSO₄ and MgCl₂ shows abnormal values may be due impurity containing in the glass vials.

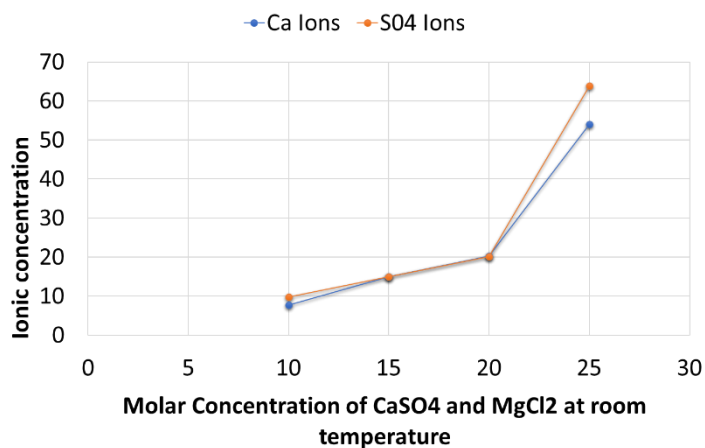


Figure 6.7 Ion Chromatography results of brines with different molar concentration at room temperature

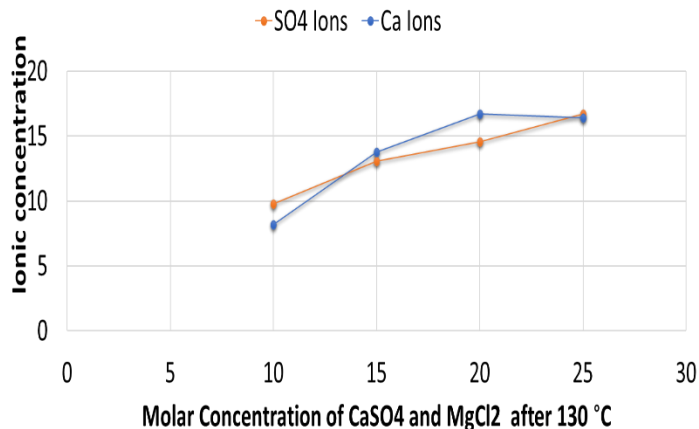


Figure 6.8 Ion Chromatography results of brines with different molar concentration after 130 °C

Ion chromatography of Smart Water containing CaSO_4 and MgCl_2 along with 2mM NaHCO_3 was done at room temperature and at 130 °C as well. The results of ion chromatography can be seen in Table 6.3 below.

Table 6.3 Ion Chromatography results of brines with different molar concentration with NaHCO_3 at room temperature and 130 °C

Smart Water (CaSO_4 and MgCl_2) with NaHCO_3				
	At room temperature		After 130°C	
Molarity	Calcium Ions	Sulphate Ions	Calcium Ions	Sulphate Ions
10 mM	13.2	11.7	12.7	10.9
15 mM	12.9	14.5	11.4	11.7
20mM	66.1	25.9	23.6	19
25 mM	29.3	24.9	17.6	16.8

The results show a high calcium and sulfate ions concentration in 10mM and 15 mM and 25 mM solution at room temperature than 130 °C as shown in Figures 6.9 and 6.10 below. Hence the values for the 20 mM solution of CaSO_4 and MgCl_2 with 2 mM NaHCO_3 shows abnormal values may be to impurities in the glass vial containing the sample.

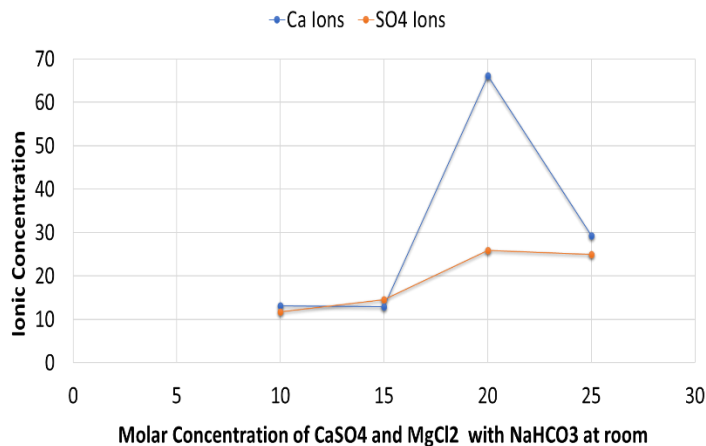


Figure 6.9 Ion Chromatography results of brines with different molar concentration with NaHCO_3 at room temperature

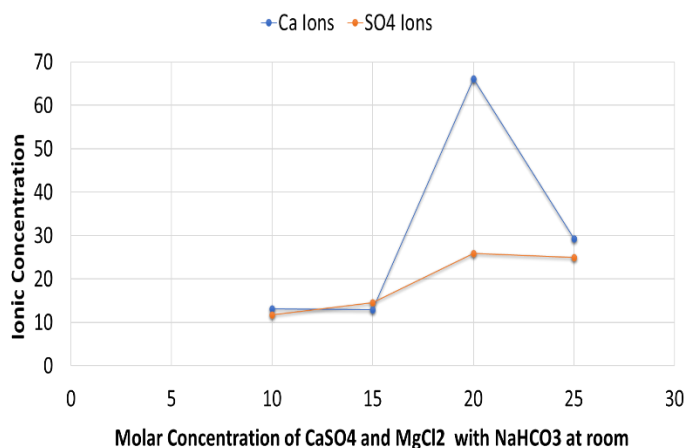
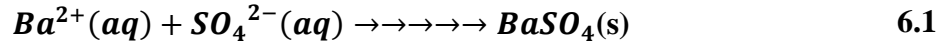


Figure 6.10 Ion Chromatography results of brines with different molar concentration with NaHCO_3 after 130 °C

6.4 Core Cleaning

A qualitative test was used for the cleaning of cores. The procedure which was followed was characterized by Puntervold (Puntervold et al. 2007). In this procedure, firstly, the cores were flooded with 5 PV de-ionized water at room temperature with a flow rate of 0.1 ml/min. The presence of SO_4^{2-} ions were tested in effluent samples.

Batch tests of the effluent were done using the BaCl_2 salt to see any precipitation of BaSO_4 . The precipitation occurs due to the reaction of Ba^{2+} ions of BaCl_2 salt with SO_4^{2-} ions present in the effluent. The reaction can be seen in Equation 6.1 below.



The precipitation of BaSO₄ changes the color of effluent samples, which can be seen in Figure 6.11.

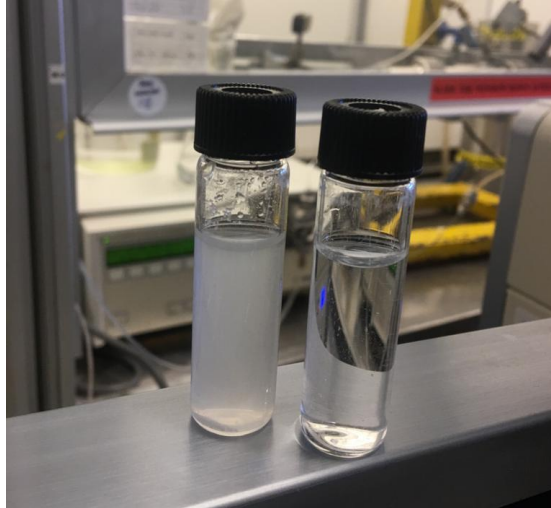


Figure 6.11 Batch test for the presence of SO₄²⁻ ions in effluent samples. Ba²⁺ ions added, confirming the formation of BaSO₄

After injection of 5 PV de-ionized water, there was no observed precipitation of BaSO₄ in the effluent samples.

6.5 Porosity and Permeability Measurement

6.5.1 Porosity Measurement

Rock porosities of all three cores were measured through Equation 6.2, and interpreted results are given in Table 6.4 below.

$$\varphi = \frac{W_{saturated}}{V_{bulk} \rho_{DI}} \quad 6.2$$

Where,

φ	Core's porosity in fraction
$W_{saturated}$	Saturated core's weight in grams
ρ_{DI}	De-ionized water's density at 20 °C in g/cm ³
V_{bulk}	Core's bulk volume in cm ³

Table 6.4 Results of Porosity Measurement

Core Name	Porosity (Fraction)
Core #1	0.4961
Core #2	0.4921
Core #3	0.4818

6.5.2 Permeability Measurement

A flooding setup was used to measure the permeabilities of rock cores. Cores were flooded at flow rates of 0.05 ml/min, 0.1 ml/min, and 0.15 ml/min with formation water, and recorded pressure differences were used to calculate permeabilities through Equation 6.3. Recorded pressure differences for corresponding flow rates and permeabilities are given in Table 6.5 below.

$$k = \frac{Q\mu L}{\Delta P A} \quad 6.3$$

Where:

k	Permeability of rock in Darcy
Q	Flow rate in ml/s
μ	Flooding fluid's viscosity in cP,
L	Core's length in cm
A	Cross-sectional flow area in cm ²
ΔP	Inlet and outlet's pressure difference in atm

Table 6.5 Results of Porosity and Permeability Measurement

Core Name	Flow Rate (ml/min)	Permeability (mD)	Average Permeability (mD)	Porosity (fraction)
Core #1	-	-	-	0.4961
Core #2	0.05 0.1 0.15	2.86 3.04 3.58	3.16	0.4921
Core #3	-	-	-	0.4818

The range of Porosity values of cores is between 0.4818 and 0.4961, while values of permeability can be measured only for one core, and the result shows average permeability of 3.16. Core #1 and #3 were drilled from the same block, and we expect a permeability in line with core #2. Results indicate that the values of porosities are high for each core while the permeability is low.

6.6 Initial core wettability

All core was restored in the same way, expecting to achieve the same core wettability. After core cleaning, core#1 was fluid restored with initial water saturation of 10% with FW, before exposure to crude oil A, by saturation with crude oil and 2 PV flooding in each direction equaling total 5PV crude oil exposure, i.e., 1 PV in start and 2PV from each side.

After Core aging, the core was SI at 130 °C using FW as imbibing brine. The results from SI test are presented in Figure 6.12.

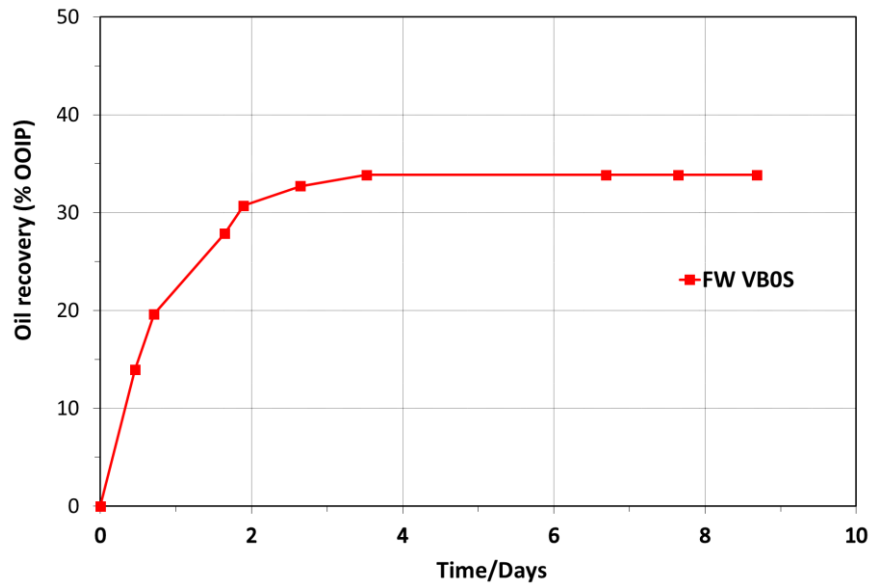


Figure 6.12 Oil recovery with spontaneous imbibition of Core#1 with FW at 130 °C

The results of spontaneous imbibition of Core #1 with FW confirms an ultimate recovery of 34 %OOIP reached after 4days. The SI results confirm that the restored Core#1 behaves soberly water wet.

6.7 Effect of Smart Water-1 in tertiary recovery mode

After 9 days, the imbibition brine was changed to Smart Water-1 (SmW-1), allowing the imbibition to continue at 130 °C. The results are presented in Figure 6.13.

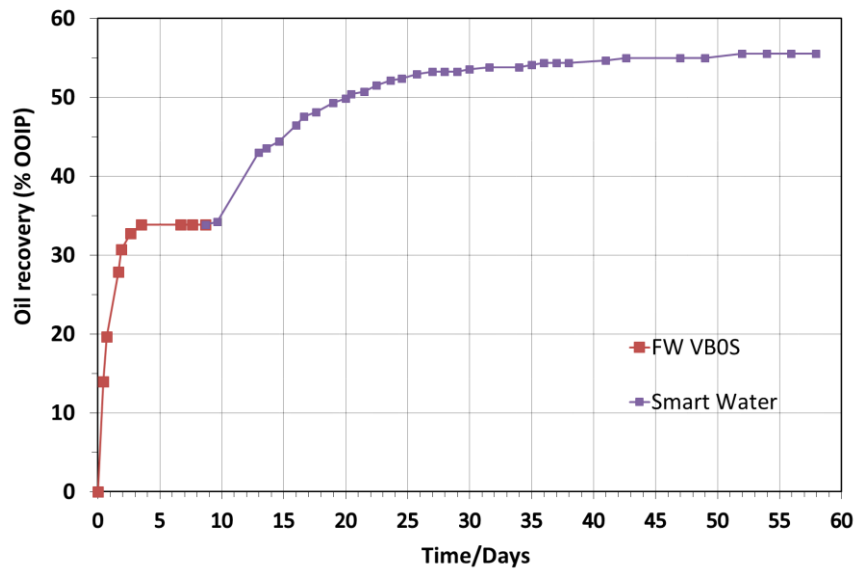


Figure 6.13 Oil recovery with spontaneous imbibition of Core#1 with FW and SmW-1 (containing 20 mM Ca^{2+} , 20 mM SO_4^{2-} , and 20mM Mg^{2+}) at 130 °C

The SI with SmW-1 containing 20 mM Ca^{2+} , 20 mM SO_4^{2-} , and 20mM Mg^{2+} was able to change core wettability, and extra oil was mobilized. A new ultimate recovery of 55 %OOIP was reached after 43 days, confirming that SmW-1 behaves as a Smart Water, and this is due to the fact that SmW-1 changes the wettability of the core.

6.8 Effect of Smart Water-1 in secondary mode

For Core #2, Smart Water-1 was used as imbibing fluid for spontaneous imbibition. The results are presented in Figure 6.14.

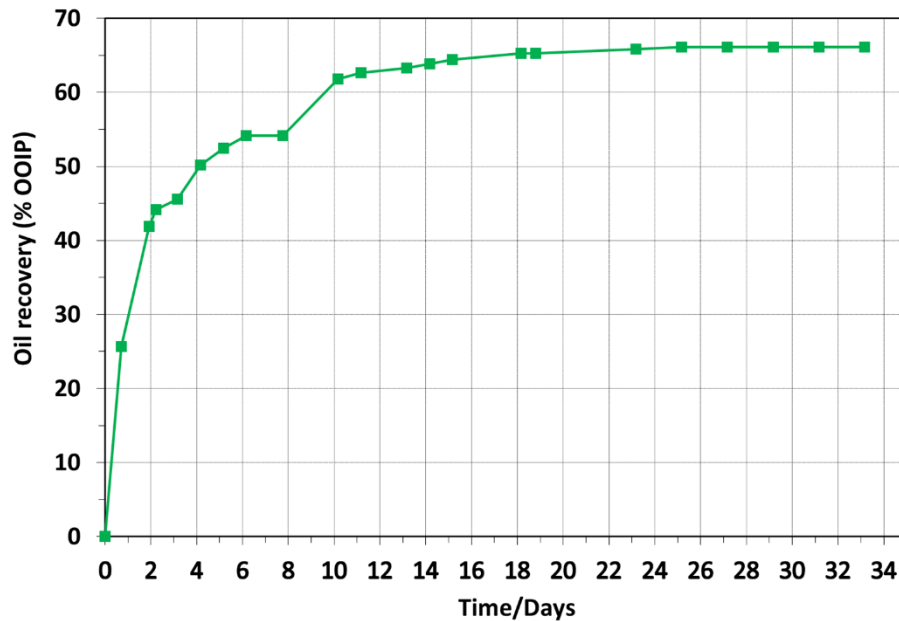


Figure 6.14 Oil recovery with spontaneous imbibition of Core#2 with SmW-1 at 130 °C

The results from SI of core #2 confirm that SmW-1 is a very efficient Smart water. The oil recovery was 42 % after 2 days which is significantly higher than observed with FW on core #1. An ultimate recovery plateau of 66.1 %OOIP was reached after 33 days, confirming that SmW-1 can change the core wettability towards more water-wet conditions.

6.9 Effect of Smart Water-2 in secondary mode

For spontaneous imbibition of Core #3, Smart Water-2 (SmW-2) was used as imbibing fluid. This brine contains 20 mM Ca^{2+} , 20 mM SO_4^{2-} , increased the Mg^{2+} concentration to 40 mM to improve the temperature stability of the brine without dramatically changing the salinity. The results is presented in Figure 6.15.

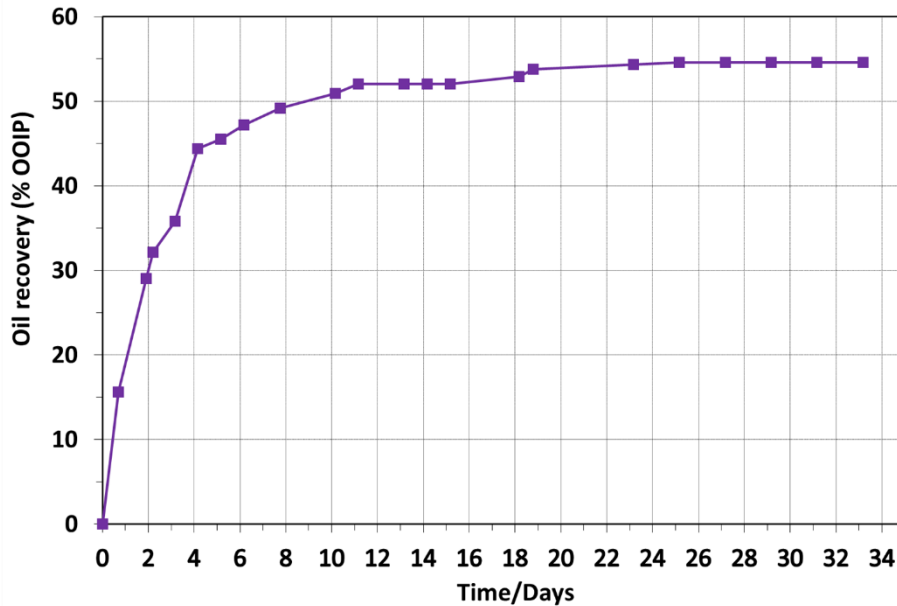


Figure 6.15 Oil recovery with spontaneous imbibition of Core#3 with SmW-2 (containing 20 mM Ca^{2+} , 20 mM SO_4^{2-} , and 40mM Mg^{2+}) at 130 °C

The results from SI of core #3 confirm that SmW-2 is less efficient than SmW-1. The oil recovery was 30 % after 2 days which is significantly higher than observed with FW on core #1 but less than SmW-1 which caused 42%. An ultimate recovery plateau of 53.8 % OOIP was reached after 33 days, confirming that increasing the concentration of Mg^{2+} in SmW-2 is able to stabilize the temperature but does not improve the wettability leading to less ultimate recovery. The less wettability alteration assumed to be due to Mg^{2+} complexes with SO_4^{2-} , hence this reduces the reactivity of SO_4^{2-} .

6.10 Wettability Measurement

To calculate the water wetness of all the three cores used, results from spontaneous imbibition of a SK chalk core that have not been exposed to crude are used as reference. The core with initial 10% S_{wi} and saturated with Heptane as oil phase. This test was performed in a previous MS thesis study by Tahmiscioglu (2020) shown in Figure 6.16.

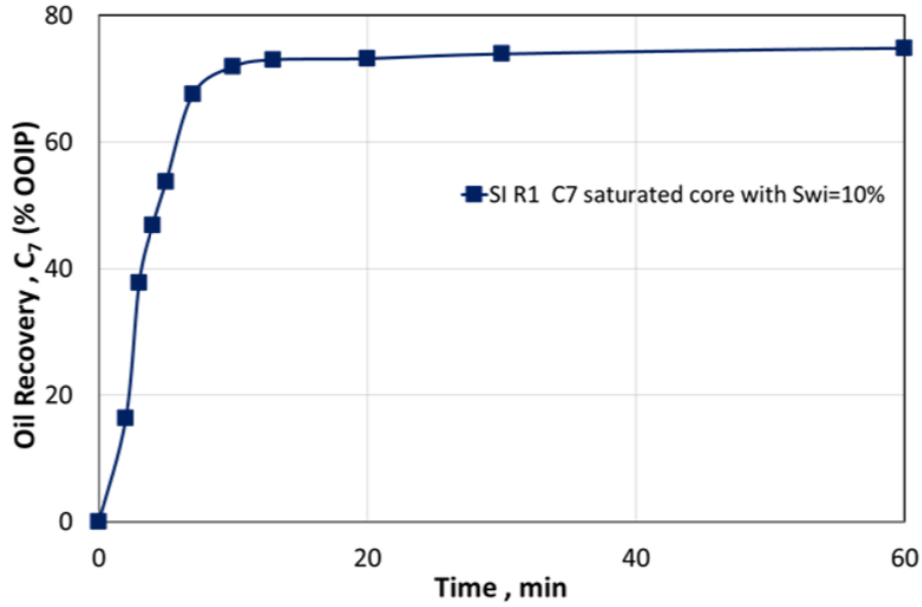


Figure 6.16 SI test results performed in a strongly water-wet SK Chalk Core (Tahmiscioglu, 2020) restored with $S_{wi} = 10\%$ and saturated with heptane

The heptane saturated core was spontaneously imbibed at 23 °C with FW. The results are shown an ultimate recovery plateau of 75%OOIP reached after 30 minutes.

The results show strong water-wet behavior and the availability of strong capillary forces for oil mobilization.

Modified Amott indices can be calculated by using Equation 6.4.

$$I_{w-SI}^* = \frac{(\%OOIP)_{test}}{(\%OOIP)_{reference}} \quad 6.4$$

Modified Amott water Indices (I_w) are similarly calculated as above and presented in Table 6.6.

Table 6.6 Modified Indices values for all three cores

	Secondary Mode		Tertiary Mode	
	Imbibing Fluid	I_{w-SI}^*	Imbibing Fluid	I_{w-SI}^*
Core #1	FW	0.452	Smart Water-1	0.734
Core #2	SmW-1	0.877		
Core #3	SmW-2	0.717		

Table 6.5 represents the water wetness of all three cores. Initial water wetness of the cores is and reproduced around 0.452. The results confirm that smart water modifies wettability towards more water-wet states in both secondary and tertiary modes.

7 Discussions

Wettability alteration is the main purpose of this study in chalk carbonate by Smart Water at a temperature of 130°C. Different ions such as SO_4^{2-} , Ca^{2+} and Mg^{2+} were used to make Smart Water. The prepared Smart Water was then used as injection brine, altering the wettability of chalk cores, making the environment more water-wet than mixed wet because the ions make water imbibe into smaller pores in carbonates. The injected brine increased the sweep efficiency of the studied system, which resulted in better Enhanced Oil Recovery (EOR) at high temperature of 130°C.

To carry out the whole procedure, first, the brines with different molar concentrations were made and then observed for any precipitation effect at 130 °C. The optimum brine (20 mM CaSO_4 and 20 mM MgCl_2) was then selected for further SI experiments to alter the wettability in Stevns Klint Chalk cores.

An Ion Chromatography test was performed on the brines to analyze the ions concentration in the brines. The test was performed at room temperature and as well as 130 °C, and the effect of precipitation on ions concentration was noted.

The porosity and permeability results of all cores used approve relatively analogous properties.

Swi of 10% was used as core restoration process initially and then by exposing the cores to equal amounts of crude oil. The crude oil, Oil A used has AN of 0.53 mgKOH/g. and BN of 0.31 mgKOH/g. Reproducible wettability results were established with FW during the SI experiments.

In the Spontaneous Imbibition process, FW provides the initial wettability on core number by producing 34% OOIP at 130 °C, before introducing the designed and selected Smart Water i.e., SmW-1. Figure 7.1 shows the effect of different brines (FW, SmW-1 in secondary and tertiary modes).

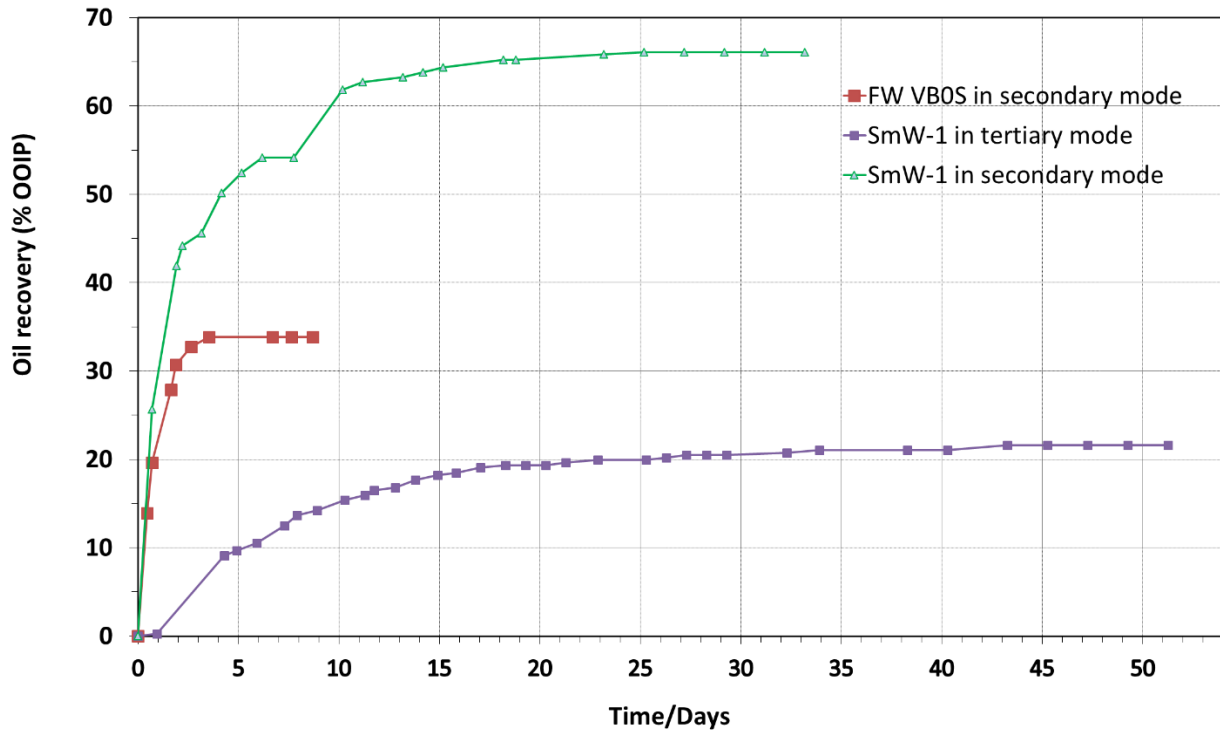


Figure 7.1 Comparison of effect of FW and SmW-1 in secondary and tertiary mode at 130 °C

The SmW-1 (Ca^{+2} , SO_4^{-2} , and Mg^{+2} 20 mM each) performs as a Smart Water in secondary and tertiary mode, altering the wettability at high temperatures in Chalk. Ca^{+2} and SO_4^{-2} ions are the key ions contributing to the wettability alteration process whereas, Mg^{+2} creates increased ionic stability of the SmW-1. Comparing, secondary mode of SmW-1 with tertiary mode in the first 10 days of SI experiment, it can be clearly seen that SmW-1 performed much better in secondary mode than in tertiary mode which indicate that the recovery is significantly fast. After first 10 days, SmW-1 has produced more than 60% of oil in secondary mode than in tertiary mode. In tertiary mode, it has produced additional 16 % after 10 days.

Now associating both Smart Waters i.e., SmW-1 and SmW-2, it is observed that SmW-1 has performed better than the SmW-2 at 130 °C. After the first 10 days of SI experiment, SmW-1 has produced more than 60 % while SmW-2 was lagging, producing around 55% as shown in Figure 7.2.

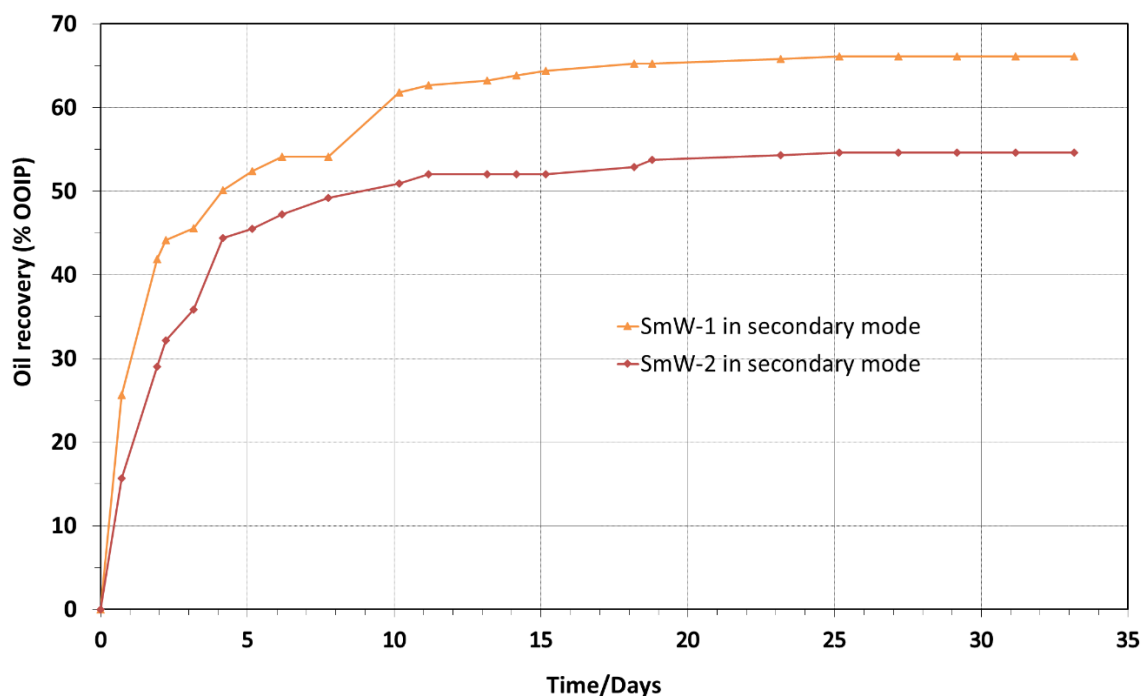


Figure 7.2 Comparison of effect of SmW-1 and SmW-2 in secondary and tertiary mode at 130 °C

The SmW-2 (Ca^{+2} , SO_4^{2-} 20 mM, and Mg^{+2} 40 mM) performed less like a Smart Water in secondary mode as compared to the SmW-1. The less wettability alteration observed is assumed to be due to Mg^{2+} complexes with SO_4^{2-} , hence reduces the reactivity of SO_4^{2-} .

Referring to Zhang (2006) work and current study results, it is prominent that Mg^{2+} is causing temperature stability in wettability alteration, and the results are more overwhelming when used with 4 times SO_4^{2-} ions.

7.1 Effect of brine composition on wettability alteration

To see the effect of brine composition on wettability alteration, the current study results of SmW-1 were compared with Tahmiscioglu (2020) as the cores used in both studies are from the same outcrop formation (Stevens Klint Chalk). The SI tests were also performed at the same temperature i.e., 130°C. The summarized data is shown in Table 7.1 below.

Table 7.1 Comparison of Secondary and Tertiary recovery results of the current study with Tahmiscioglu (2020) work at 130°C

Mode	Imbibing Fluid		
	%OOIP by SmW-1 at 130 °C	SW %OOIP at °C	%OOIP by CaSO ₄ (10 mM) at °C
Secondary	66.1	58.1	29.6
Tertiary	55.5	53.8	40.1

It can be clearly seen that the current research results are better than the previous Tahmiscioglu (2020) results. Referring to both Smart Waters, SmW-1 and 10 mM CaSO₄ used by Tahmiscioglu, it is observed that SmW-1 used in this study has produced 15.5% more oil in tertiary mode than the Smart Water used in the previous work (Tahmiscioglu, 2020) as seen in Figure 7.3 and Figure 7.4 below.

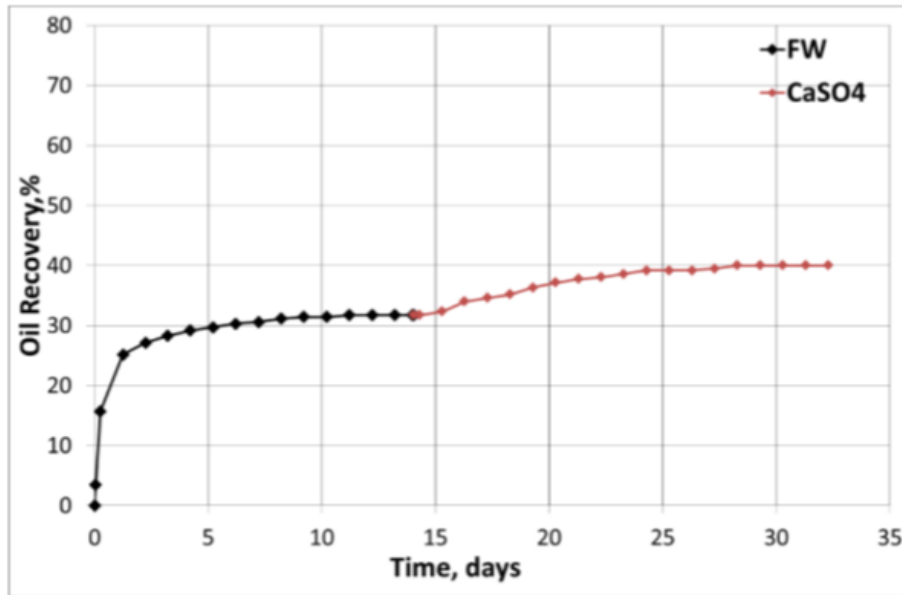


Figure 7.3 Oil Recovery with SI by FW and 10 mM CaSO₄ in Core #1 at 130 C (Tahmiscioglu, 2020)

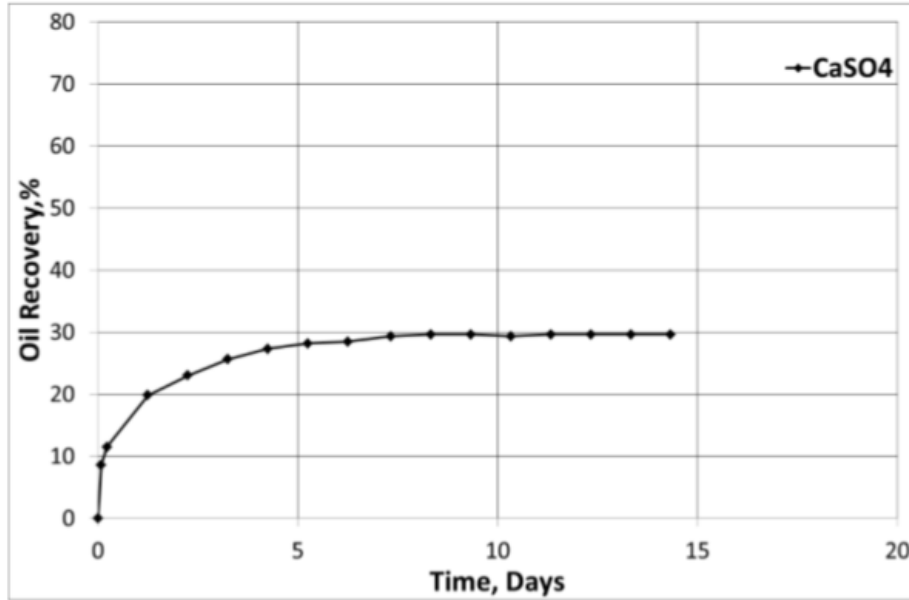


Figure 7.4 Oil Recovery with SI by 10 mM CaSO₄ at 130°C (Tahmiscioglu, 2020)

Comparison of SmW-1 with the Sea Water in tertiary and secondary mode, used by Tahmiscioglu (2020) was observed to see the effect of wettability alteration by both brines as shown in figure 7.5 and figure 7.6. The SmW-1 used in this study excelled the SW by almost 8% in secondary mode and 1.7% in tertiary mode due to increased concentration of Ca⁺² and SO₄⁻² ions.

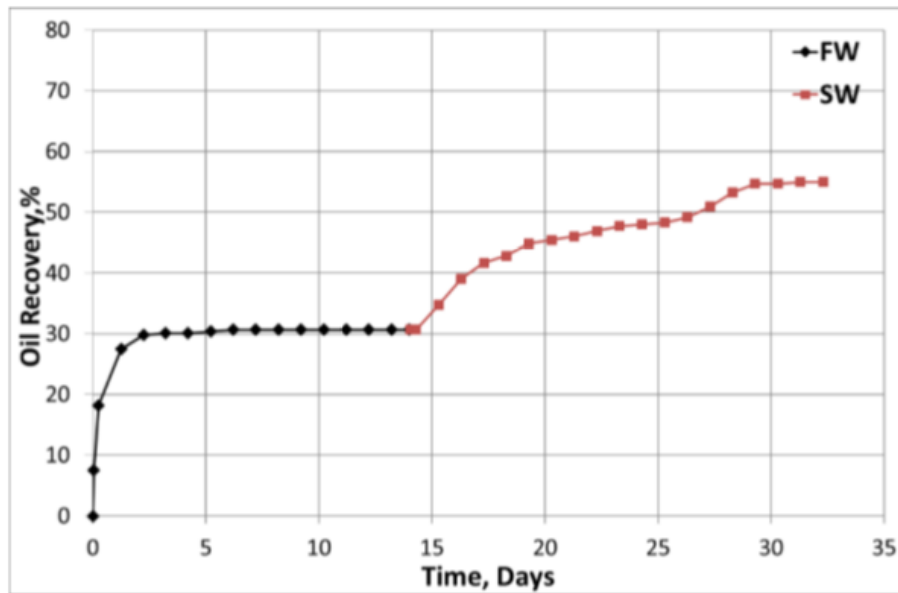


Figure 7.5 Oil Recovery with SI by FW-SW in Core#6 at 130°C (Tahmiscioglu, 2020)

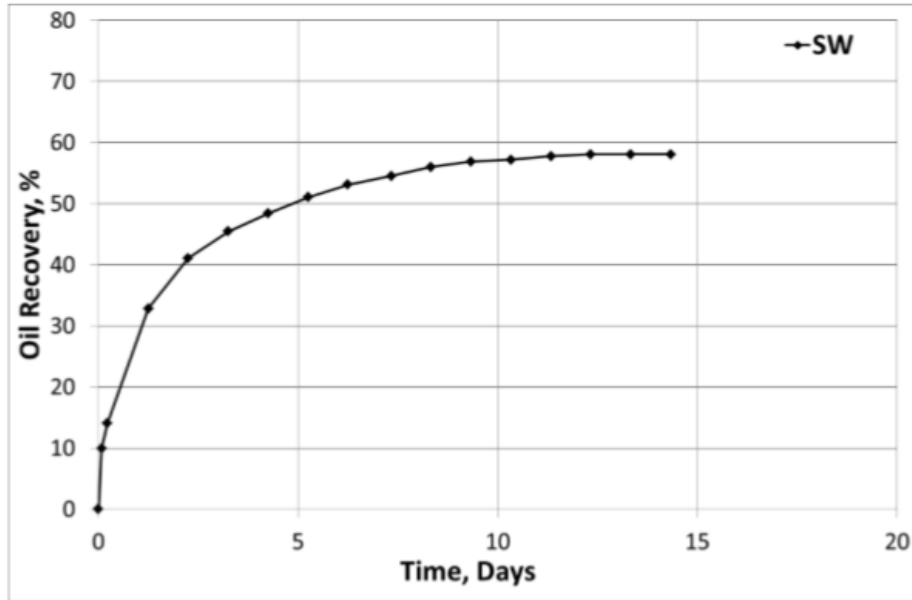


Figure 7.6 Oil Recovery with SI by SW in Core #2 at 130°C (Tahmiscioglu, 2020)

The results of the SW from the Tahmiscioglu's thesis (2020) were observed and compared with the current study as the cores are used from the same outcrop formation (Stevns Klint Chalk). The results from the Tahmiscioglu's work (2020) validate that SW is an efficient Smart Water in Chalk at 130°C, which changes the core wettability towards more water-wet conditions.

However, the comparison of the results of SW and SmW-1 clearly shows that the Smart Water used in this study has increases the wettability alteration, than the SW during the SI experiment because of low salinity.

7.2 Reactivity effect of temperature and brine composition.

To see the reactivity effect of brine composition and temperature on wettability alteration, the current study results of SmW-1 at 130 °C were compared with Andreassen (2019). The comparison made The Smart Water composition used by Andreassen (2019) was 10 mM CaSO₄ and at 70 °C. The summarized data is shown in table 7.2 below.

Table 7.2 Comparison of Secondary recovery results of the current study with Andreassen (2019) work

Mode	Imbibing Fluid		
	%OOIP by SmW-1 (20 mM CaSO ₄ and 20 mM MgCl ₂) at 130 °C	%OOIP by SW at 70 °C	%OOIP by CaSO ₄ . 2 H ₂ O (13 mM) at 70 °C
Secondary	66.1	9	11

Referring to both Smart Waters i.e., SmW-1 (20mM CaSO₄ and 20 mM MgCl₂) and 13 mM CaSO₄.2H₂O, it can be seen that SmW-1 used in this study has produced 55.1% more oil in secondary mode than the Smart Water used in the previous work (Andreassen, 2019) as seen in Figure 7.7 below. It is visible that the research results of this study are better than the previous Andreassen (2019) results.

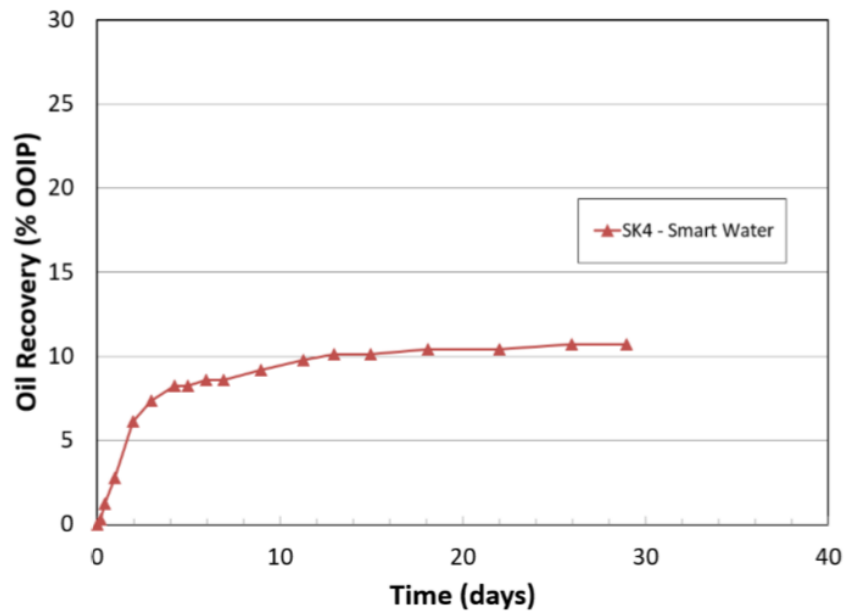


Figure 7.7 Oil Recovery with SI by Smart Water 13 mM CaSO₄ at 70 °C in Core #SK4 (Andreassen, 2019)

Now comparing with the Sea Water, the SmW-1 used in this study excelled the SW by almost 57% in secondary mode, as seen in Figure 7.8 below. The SmW-1 performed better because of high temperature EOR.

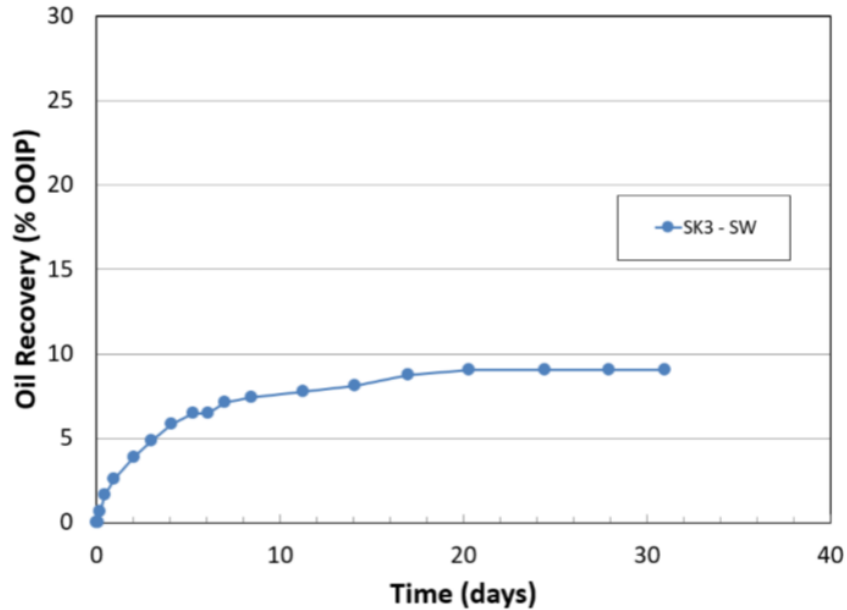


Figure 7.8 Oil Recovery with SI by SW at 70°C in Core #SK3 (Andreassen, 2019)

The research results of this study are compared with the previous Andreassen (2019) study and the results of this study show relatively high ultimate recovery due to improved wettability alteration and increased ionic concentration of SmW-1 at 130°C. The current study results of SmW-1 at 130 °C were also compared with Lindanger (2019), to see the reactivity effect of brine composition and temperature on wettability alteration, The Smart Water composition used by Lindanger (2019), was 13 mM CaSO₄ at 90 °C. The summarized data is shown in Table 7.3 below.

Table 7.3 Comparison of Secondary recovery results of the current study with Lindanger (2019) work

Mode	Imbibing Fluid		
	%OOIP% with Smart Water (20mM CaSO ₄ and 20 mM MgCl ₂)	%OOIP with Sea Water at 90 °C	%OOIP with 13 mM CaSO ₄ at 90 °C
Secondary	66.1	23	27

Referring to both Smart Waters i.e., SmW-1 (20mM CaSO₄ and 20 mM MgCl₂) and Smart Water used by Lindanger (2019) (13 mM CaSO₄), it is visible that Smart Water used in this study has

produced 39.1% more oil in secondary mode than the Smart Water used in the previous work (Lindanger, 2019) as seen in Figure 7.9 below. The argument for this is that the increases ionic concentration and high temperature causing more wettability alteration than the previous Lindanger (2019) results.

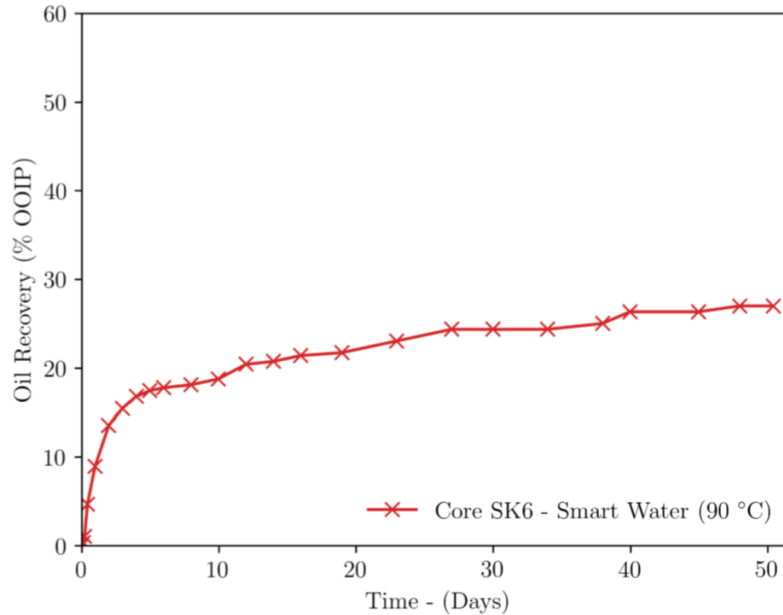


Figure 7.9 Oil Recovery with SI by Smart Water in Core #SK6 at 90 °C (Lindanger, 2019)

Now comparing with the Sea Water, the Smart Water, SmW-1 used in this study excelled the SW by almost 43.1% in secondary mode, as seen in Figure 7.10 below. This is because the composition and temperature, both are different in the current study, hence causing more wettability alteration effects.

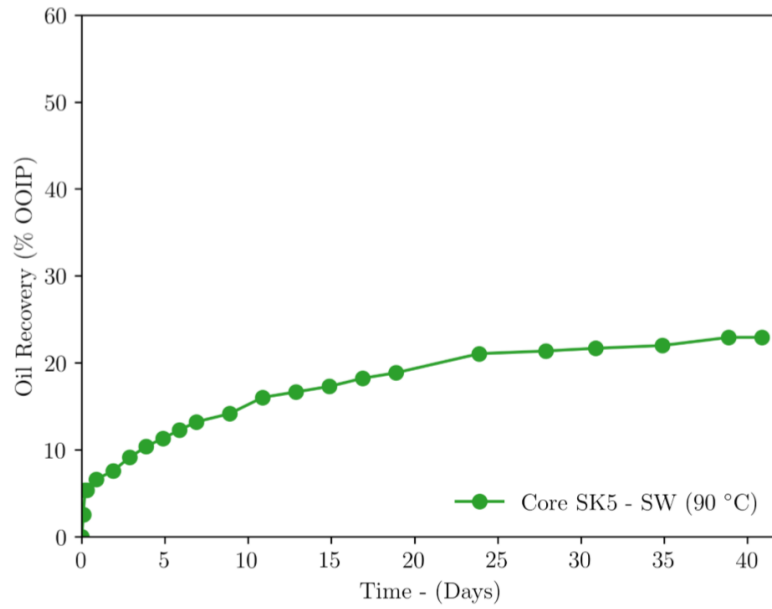


Figure 7.10 Oil Recovery with SI by SW in Core #SK5 at 90 °C (Lindanger, 2019)

The reason for improved results of wettability alteration in this study in comparison to Lindanger, 2019, is that the concentration of ions is higher for this study than the previous, as well as the temperature.

8 Conclusion

The main objectives of the study had focus on initial wettability, wettability alteration with smart water and brine stability at high 130° C.

FW was used as a spontaneous imbibition fluid in secondary mode to observe the initial wettability. The SI test of FW produced 34% of oil for Core No. 1 which indicates a significant water-wet state of the core.

Then a solution of CaSO₄ and MgCl₂ having molarity of 20mM each is used as a Smart Water that can cause wettability alteration at 130°C in the outcrop cores of chalk and it confirmed the wettability alteration in secondary and as well as tertiary mode.

The Smart Water termed, SmW-1 (Ca²⁺, SO₄²⁻ and Mg²⁺ 20 mM each) was introduced in tertiary mode subsequently in the same core, which resulted in extra oil recovery of 21.5 %OOIP. This shows an improved Smart Water characteristic when compared with the SW study carried out by Tahmiscioglu (2020).

SmW-1 was used as a spontaneous imbibing fluid in a secondary mode which recovered oil of 66.1%. This result is overwhelming and shows a high potential for EOR effects.

The smart Water termed, SmW-2 of double magnesium content (20mM CaSO₄ and 40 mM MgCl₂) was used in secondary mode to see the effects of increased Mg²⁺ ions as the SW contained 45 mM of Mg²⁺ ions. The SI resulted in 54.6% of OOIP oil recovery.

The results of SI of SmW-1 are significantly encouraging and could be potentially used in Chalk reservoirs of the North Sea, after a further study of the brine ionic stability at high temperature. Typical reservoirs that can be benefitted by this study are Ekofisk, Tor and Hod fields, having almost the same high temperature.

8.1 Future Work

In the current study, it is assumed that Ca^{2+} is precipitating around the core rim, prohibiting further recovery of oil. It is known that Ca^{2+} causes less precipitation at low temperature (e.g., 70 °C), so the same SmW-1 should be tested at 70 °C and/or 90 °C to see its efficiency.

Mg^{2+} could be introduced higher than 20 mM but in a step by step manner to minimize the complexity with SO_4^{2-} ions.

As we know, SW has more SO_4^{2-} ions (24mM) than the Smart Waters we designed in the lab (20 mM), the increased concentration of SO_4^{2-} ions could be added to the brine composition to see its effect.

The experimental work performed in this study should be validated to confirm the obtained results.

Bibliography

- Ahr, W. M. (2011). Geology of carbonate reservoirs: the identification, description, and characterization of hydrocarbon reservoirs in carbonate rocks. John Wiley & Sons.
- Al-Maamari, R. S. H., & Buckley, J. S. (2013). Asphaltene Precipitation and Alteration of Wetting: The Potential for Wettability Changes during Oil Production. SPE reservoir evaluation & engineering, 6(4), 210-214. <https://doi.org/10.2118/84938-pa>.
- Alvarez, J. M., & Sawatzky, R. P. (2013, 2013/6/11/). Waterflooding: Same Old, Same Old? SPE Heavy Oil Conference-Canada, Calgary, Alberta, Canada. <https://doi.org/10.2118/165406-MS>.
- Anderson, W. G. (1986). Wettability Literature Survey- Part 1: Rock/Oil/Brine Interactions and the Effects of Core Handling on Wettability. Journal of petroleum technology, 38(10), 1125-1144. <https://doi.org/10.2118/13932-PA>.
- Andreassen, E. (2019). Production of Smart Water by Acid Flooding in Chalk: Temperature Limitation at Slightly Water-Wet Conditions. MS thesis. University of Stavanger.
- Austad, T. & Milter, J. (1997). Spontaneous Imbibition of Water Into Low Permeable Chalk at Different Wettabilities Using Surfactants. Houston, Texas. <https://doi.org/10.2118/37236-MS>.
- Austad, T., Strand, S., Madland, M. V., Puntervold, T., & Korsnes, R. I. (2007). Seawater in chalk: An EOR and compaction fluid. International petroleum technology conference. International Petroleum Technology Conference.
- Buckley, J. S. (1996). Mechanisms and consequences of wettability alteration by crude oils. Department of Petroleum Engineering, Heriot-Watt University. Edinburgh.
- Buckley, J. S., & Liu, Y. (1998). Some mechanisms of crude oil/brine/solid interactions. Journal of Petroleum Science and Engineering, 20(3), 155-160. [https://doi.org/https://doi.org/10.1016/S0920-4105\(98\)00015-1](https://doi.org/https://doi.org/10.1016/S0920-4105(98)00015-1)
- Buckley, J. S., Takamura, K., & Morrow, N. R. (2013). Influence of Electrical Surface Charges on the Wetting Properties of Crude Oils. SPE reservoir engineering, 4(3), 332-340. <https://doi.org/10.2118/16964-pa>

- Chilingar, G. V., & Yen, T. F. (1983). Some Notes on Wettability and Relative Permeabilities of Carbonate Reservoir Rocks, II. Energy Sources, 7(1), 67-75. <https://doi.org/10.1080/00908318308908076>
- Cook, T. A. (2013). Reserve growth of oil and gas fields—Investigations and applications [Report](2013-5063). (Scientific Investigations Report, Issue. U. S. G. Survey. <http://pubs.er.usgs.gov/publication/sir20135063>
- Craig, F. F. (1971). The reservoir engineering aspects of waterflooding (Vol. vol. 3). Henry L. Doherty Memorial Fund of AIME.
- Denekas, M. O., Mattax, C. C., & Davis, G. T. (1959). Effects of Crude Oil Components on Rock Wettability. Transactions of the AIME, 216(01), 330-333. <https://doi.org/10.2118/1276-G>
- Fathi, S. J., Austad, T., & Strand, S. (2011). Water-Based Enhanced Oil Recovery (EOR) by “Smart Water”: Optimal Ionic Composition for EOR in Carbonates. Department of Petroleum Engineering, Faculty of Science and Technology, University of Stavanger, 4036 Stavanger, Norway.
- Green, D. W., & Willhite, G. P. (1998). Enhanced oil recovery (Vol. vol. 6). Henry L. Doherty Memorial Fund of AIME, Society of Petroleum Engineers.
- Grotzinger, J. and Jordan, T. H. (2014). Understanding Earth. W. H. Freeman. isbn: 9781319129859.
- Hall. (1961). Analysis of gravity drainage. In: AIME: Journal of Petroleum Technology 13.09, pp. 927–936. <https://doi.org/10.2118/1517-G-PA>.
- Hirasaki, G. J. (1991). Wettability: Fundamentals and Surface Forces. SPE formation evaluation, 6(2), 217-226. <https://doi.org/10.2118/17367-PA>
- Jadhunandan, P. P., & Morrow, N. R. (2013). Effect of Wettability on Waterflood Recovery for Crude-Oil/Brine/Rock Systems. SPE reservoir engineering, 10(1), 40-46. <https://doi.org/10.2118/22597-pa>.
- Kowalewski, E., Boassen, T., & Torsæter, O. (2003). Wettability alterations due to aging in crude oil; wettability and Cryo-ESEM analyses. Journal of Petroleum Science and Engineering - J PET SCI ENGINEERING, 39, 377-388. [https://doi.org/10.1016/S0920-4105\(03\)00076-7](https://doi.org/10.1016/S0920-4105(03)00076-7)
- Letellier, P., Mayaffre, A., & Turmine, M. (2007). Drop size effect on contact angle explained by nonextensive thermodynamics. Young's equation revisited. Journal of Colloid and

- Lindanger, M. (2019). Production of Smart Water by Acid Flooding in Chalk Cores: Oil Recovery Effects at Intermediate Temperature. MA thesis. University of Stavanger.
- Menezes, J., Yan, J., & Sharma, M. (1989). The Mechanism of Wettability Alteration Due to Surfactants in Oil-Based Muds. <https://doi.org/10.2118/18460-MS>
- Moore, T. F., & Slobod, R. L. (1955, 1955/1/1/). Displacement of Oil by Water-Effect of Wettability, Rate, and Viscosity on Recovery Fall Meeting of the Petroleum Branch of AIME, New Orleans, Louisiana. <https://doi.org/10.2118/502-G>
- Muggeridge, A., Cockin, A., Webb, K., Frampton, H., Collins, I., Moulds, T., & Salino, P. (2014). Recovery rates, enhanced oil recovery and technological limits. *Philos Trans A Math Phys Eng Sci*, 372(2006), 20120320-20120320. <https://doi.org/10.1098/rsta.2012.0320>.
- Muskat, M. (1949). Physical principles of oil production. English. New York: McGraw Hill Book Co.
- Pierre, A., Lamarche, J. M., Mercier, R., Foissy, A., & Persello, J. (1990). CALCIUM AS POTENTIAL DETERMINING ION IN AQUEOUS CALCITE SUSPENSIONS. *Journal of Dispersion Science and Technology*, 11(6), 611-635. <https://doi.org/10.1080/01932699008943286>.
- Punternvold, T. (2008). Waterflooding of carbonate reservoirs: EOR by wettability alteration [University of Stavanger, Faculty of Science and Technology, Department of Petroleum Engineering]. Stavanger.
- Punternvold, T., Strand, S., and Austad, T. (2007). New Method To Prepare Outcrop Chalk Cores for Wettability and Oil Recovery Studies at Low Initial Water Saturation. In: *Energy & Fuels - ENERGY FUEL* 21. doi: 10.1021/ef700323c.
- Standnes, D. C. (2001). Enhanced oil recovery from oil-wet carbonate rock by spontaneous imbibition of aqueous surfactant solutions [Norges teknisk-naturvitenskapelige universitet, Petroleumsteknologi og anvendt geofysikk]. Trondheim.
- Strand, S. (2005). Wettability alteration in chalk: a study of surface chemistry [University of Stavanger]. Stavanger.
- Strand, S., Høgnesen, E. J., & Austad, T. (2006). *Colloids Surf, A*, 275, 1.

- Strand, S., Puntervold, T., & Austad, T. (2008). Effect of Temperature on Enhanced Oil Recovery from Mixed-Wet Chalk Cores by Spontaneous Imbibition and Forced Displacement Using Seawater. *Energy & Fuels*, 22(5), 3222-3225. <https://doi.org/10.1021/ef800244v>.
- Tahmiscioglu, A. N., (2020). Optimized Smart Water Composition at Ekofisk Conditions-Oil Recovery at High Temperatures. MS thesis. University of Stavanger.
- Torrijos, I. D. Pinerez, Sæby, K. G., Strand, S., and Puntervold, T. (2019). Impact of Temperature on Wettability Alteration by Smart Water in Chalk”. In: IOR 2019 20th European Symposium on Improved Oil Recovery.
- Treiber, L. E., & Owens, W. W. (1972). A Laboratory Evaluation of the Wettability of Fifty OilProducing Reservoirs. *Society of Petroleum Engineers journal*, 12(6), 531-540. <https://doi.org/10.2118/3526-PA>.
- Wade, J. E. (1971, 1971/1/1/). Some Practical Aspects of Waterflooding 8th World Petroleum Congress, Moscow, USSR. <https://doi.org/>
- Yuan, Y., & Lee, T. R. (2013). Contact Angle and Wetting Properties. In G. Bracco & B. Holst (Eds.), *Surface Science Techniques* (pp. 3-34). Springer Berlin Heidelberg. https://doi.org/10.1007/978-3-642-34243-1_1.
- Zhang, P. (2006). Water-based EOR in fractured chalk: wettability and chemical additives University of Stavanger, Faculty of Science and Technology, Department of Petroleum Engineering. Stavanger.
- Zhang, P., & Austad, T. (2006). *Colloids Surf., A*, 279, 179.
- Zhang, P., Tweheyo, M. T., & Austad, T. (2007a). *Colloids Surf., A*, 301, 199.
- Zhang, P., Tweheyo, M. T., & Austad, T. (2007b). Wettability alteration and improved oil recovery by spontaneous imbibition of seawater into chalk: Impact of the potential determining ions: Ca^{2+} , Mg^{2+} and SO_4^{2-} . *Colloids Surf., A*, 301, 199.
- Zolotukhin, & Anatolij, B. (2000). Introduction to petroleum reservoir engineering. eng. Kristiansand.

Appendixes

Brine Recipes

Salt	SSW (g/l)	VB0S (g/l)	Smart Water-1 (g/l)	Smart Water-2 (g/l)
NaCl	23.38	57.70	0.00	0.00
Na₂SO₄	3.41	0.00	0.00	0.00
KSCN	0.00	0.00	0.00	0.00
NaHCO₃	0.17	0.781	0.00	0.00
KCl	0.75	0.395	0.00	0.00
MgCl₂×6H₂O	9.05	1.58	4.066	8.132
CaCl₂×2H₂O	1.91	4.26	0.00	0.00
BaCl₂×2H₂O	0.00	0.00	0.00	0.00
SrCl₂×6H₂O	0.00	0.00	0.00	0.00
CaSO₄×2H₂O	0.00	0.00	2.73	2.73
Density (g/cm³)	1.024	1.041	0.00	0.00
TDS (g/L)	33.39	62.83	0.00	0.00

Core # 1 Spontaneous Imbibition Data for FW in secondary mode

Time (days)	Recovery (ml)	Recovery % OOIP)
0.0	0.0	0.0
0.46	4.9	13.9
0.71	6.9	19.6
1.65	9.8	27.9
1.90	10.8	30.7
2.65	11.5	32.7
3.52	11.9	33.9
6.69	11.9	33.9
7.65	11.9	33.9
8.69	11.9	33.9

Core # 1 Spontaneous Imbibition Data for SmW-1 in tertiary mode

Time (days)	Recovery (ml)	Recovery % OOIP)
0.00	0.0	0.0
0.95	0.1	0.3
4.29	3.2	9.1
4.92	3.4	9.7
5.92	3.7	10.5
7.29	4.4	12.5
7.92	4.8	13.7
8.92	5.0	14.2
10.29	5.4	15.4
11.29	5.6	15.9
11.75	5.8	16.5
12.79	5.9	16.8
13.79	6.2	17.6
14.92	6.4	18.2
15.83	6.5	18.5
17.04	6.7	19.1
18.29	6.8	19.3
19.29	6.8	19.3
20.29	6.8	19.3
21.29	6.9	19.6
22.88	7.0	19.9
25.29	7.0	19.9

26.29	7.1	20.2
27.29	7.2	20.5
28.29	7.2	20.5
29.29	7.2	20.5
32.29	7.3	20.8
33.92	7.4	21.1
38.29	7.4	21.1
40.29	7.4	21.1
43.25	7.6	21.6
45.25	7.6	21.6
47.25	7.6	21.6
49.25	7.6	21.6
51.25	7.6	21.6

Core # 2 Spontaneous Imbibition Data for SmW-1 in secondary mode

Time (days)	Recovery (ml)	Recovery % OOIP)
0.0	0.0	0.0
0.71	9.0	25.6
1.92	14.7	41.9
2.21	15.5	44.2
3.17	16.0	45.6
4.17	17.6	50.1
5.17	18.4	52.4
6.17	19.0	54.1
7.75	19.0	54.1
10.17	21.7	61.8
11.17	22.0	62.7
13.17	22.2	63.2
14.17	22.4	63.8
15.17	22.6	64.4
18.17	22.9	65.2
18.79	22.9	65.2
23.17	23.1	65.8
25.17	23.2	66.1
27.17	23.2	66.1
29.17	23.2	66.1
31.17	23.2	66.1
33.17	23.2	66.1

Core # 3 Spontaneous Imbibition Data for SmW-2 in secondary mode

Time (days)	Recovery (ml)	Recovery % OOIP)
0.0	0.0	0.0
0.71	5.5	15.6
1.92	10.2	29.0
2.21	11.3	32.1
3.17	12.6	35.8
4.17	15.6	44.4
5.17	16.0	45.5
6.17	16.6	47.2
7.75	17.3	49.2
10.17	17.9	50.9
11.17	18.3	52.1
13.17	18.3	52.1
14.17	18.3	52.1
15.17	18.3	52.1
18.17	18.6	52.9
18.79	18.9	53.8
23.17	19.1	54.3
25.17	19.2	54.6
27.17	19.2	54.6
29.17	19.2	54.6
31.17	19.2	54.6
33.17	19.2	54.6